Rock Properties and Sealing Efficiency in Fine-grained Siliciclastic Caprocks

— Implications for CCS and Petroleum Industry

Mohammad Nooraiepour

Dissertation submitted for the degree of Philosophiae Doctor
Department of Geosciences
Faculty of Mathematics and Natural Sciences
University of Oslo
September 2018

Series of dissertations submitted to the
Faculty of Mathematics and Natural Sciences, University of Oslo
No. 2061

ISSN 1501-7710

Cover: Hanne Baadsgaard Utigard.
Print production: Reprosentralen, University of Oslo.

Preface

This dissertation has been submitted to the Department of Geosciences at the Faculty of Mathematics and Natural Sciences at the University of Oslo in accordance with the requirements for the degree of Philosophiae Doctor (Ph.D.). The study was conducted as a part of the FME SUCCESS Centre: subsurface CO_2 storage — critical elements and superior strategies. The SUCCESS, a center of environment-friendly energy research (FME), is funded by the Research Council of Norway with a consortium of partners from universities, research institutes, and industries.
This dissertation follows the Manuscript Document Format and is organized in two main parts and an appendix. In the first part, the motivations and objectives, relevant scientific background, summary and outcomes of the research, and concluding remarks are presented. The second part includes the published articles and submitted manuscripts. The results of the Ph.D. research have contributed to scientific knowledge in terms of five manuscripts (from now on referred to as Paper), of which I am the first author of all five. In part one (chapter 4), a self-contained overview and summary of the most important findings of the papers are given. The extended abstracts and conference proceedings are enclosed at the end of the dissertation in the appendix.

Mohammad Nooraiepour, Oslo, August 2018

Abstract

CO_2 sequestration in geological formations is a promising technology and a crucial measure to reduce CO_2 emissions across the energy system. It is an essential part of the solution for mitigating climate change caused by anthropogenic greenhouse gases. Three principal criteria are required for the selection of a geological storage site: storage capacity, injectivity, and containment. This dissertation primarily focuses on the CO_2 containment and properties of fine-grained siliciclastic caprocks. The outcomes of the research, however, are also partly applicable for injectivity assessments. The dissertation has embraced multiscale approach (pore-, core-, and field-scale), multidisciplinary techniques, and includes a number of carefully selected experimental and analytical investigations. The research contributes to the existing knowledge of caprock sequences and reduces some of the uncertainties associated with the assessment of containment efficiency for geological CO_2 storage sites. It also provides answers to some of the less-investigated questions regarding the CO_2–brine–rock interactions, and geophysical monitoring during a potential upward leakage of the CO_2 plume. The first part of the study explores depositional and compaction trends and their effect on the evolution of rock properties in fine-grained clastic sediments. It presents examples from the caprock sequences in the SW Barents Sea and the North Sea. Salt precipitation in the fractured caprocks was the second investigated question. We designed and fabricated a high-pressure high-temperature microfluidic pressure vessel to house geomaterial micromodels. Moreover, we introduced a conceptual framework that suggests salt precipitation is not only a near wellbore phenomenon but also a sealing mechanism that can impede CO_2 leakage from the fracture networks. Finally, we have studied how acoustic velocity and electrical resistivity may be influenced by dominant fracture flow of brine–CO_2 system to simulate changes in geophysical properties during a potential CO_2 leakage. In addition to the carbon capture and storage (CCS), researchers in the petroleum industry, waste repositories, and water resources can also be benefited from the outcomes of this dissertation.

Acknowledgments

First and foremost, I would like to express my sincere appreciation to my supervisors, Associate Professor Nazmul Haque Mondol and Associate Professor Helge Hellevang, for the invaluable motivation, support, and knowledge. This fantastic journey for me as a PhD student was an opportunity to experience, learn, and develop and I owe them a great deal of gratitude. Thank you for your enthusiasm and dedication to scientific research that inspired me, and helped me build confidence and independence as a young researcher.

I am deeply thankful to the petroleum geomechanics and geophysics department, and rock mechanics laboratory at the Norwegian Geotechnical Institute (NGI). The expertise, technical assistance, and professional and personal qualities were extraordinary. Lars Grande, Magnus Soldal, Heidi Debreczeny Wilkinson, Dr. Guillaume Sauvin, Dr. Elin Skurtveit, and Bjørnar Slensvik – thank you all. I am, particularly, indebted to Dr. Joonsang Park and Dr. Bahman Bohloli for their time, support, and contributions.

Over my years at the University of Oslo, it has been a great experience to be part of the Department of Geosciences, and the inspiring CO_2 storage research group. I wish to thank all the members for the good spirit, generous support, and continuous friendship. I had the pleasure to enjoy numerous talks and conversations, about both technical and non-technical subjects. I would like to thank Professor Emeritus Knut Bjørlykke, Professor Emeritus Per Aagaard, Professor Jens Jahren, and Dr. Manzar Fawad. Gudmund Dalsbø thank you for all your help and support, and especially for the Friday-afternoon-reminders. I appreciate Mufak Said Naoroz, Siri Simonsen, Berit Løken Berg, and Thor Axel Thorsen for the technical support and assistance. Endless gratitude for the companionship to the skilled and cheerful friends, collogues, and officemates: Irfan, Beyene, Christian, Honore, Oluwakemi, Aatisha, Lamech, Jørgen, Mark, Johnathon, and Ulrich. Salah Akhavan, Rohaldin, Mohammad, and Javad thank you for the delightful Persian gatherings, coffee times, and your friendship and insights. Hossein Fazeli – you are an incredible friend, collogue, and researcher.

Finally, I would like to mention my loved ones. To Reihaneh, my wife, for her love, encouragement, and all heart-warming support and patience in the past intensive couple of months. Thank you for being who you are. Most profound gratitude to my mom and dad, Mehran and Hossein, for being such wonderful parents and kind friends. You sacrificed a lot, provided me unique opportunities, believed in me, and supported me with your love and wisdom. My siblings, Alireza and Amin, you are genuinely excellent brothers. Thank you for always being there for me.

I also would like to express my gratitude to the Department of Geosciences at UiO, Research Council of Norway, and the SUCCESS center for financial support of this PhD fellowship and hosting me. The research was also benefited from the support of the SealCap project (shale rock properties and sealing capacity in the SW Barents Sea area) funded by Eni Norge, and PROTECT project (protection of caprock integrity for large-scale CO_2 storage) funded by Research Council of Norway and industry partners.

Mohammad Nooraiepour, Oslo, August 2018

List of Papers

This dissertation includes the following articles:

Paper A: Experimental mechanical compaction of reconstituted shale and mudstone aggregates: Investigation of petrophysical and acoustic properties of SW Barents Sea cap rock sequences
M. Nooraiepour, N.H. Mondol, H. Hellevang, and K. Bjørlykke
Published, *Marine and Petroleum Geology*, 2017, 80, 265-292

Paper B: Permeability and physical properties of semi-compacted fine-grained sediments —a laboratory study to constrain mudstone compaction trends
M. Nooraiepour, N.H. Mondol, H. Hellevang
Resubmitted to *Marine and Petroleum Geology*, 2018

Paper C: Compaction and mechanical strength of Middle Miocene mudstones in the Norwegian North Sea —the major seal for the Skade CO_2 storage reservoir
M. Nooraiepour, B.G. Haile, H. Hellevang
Published, *International Journal of Greenhouse Gas Control*, 2017, 67, 49-59

Paper D: Effect of CO_2 phase states and flow rate on salt precipitation in shale caprocks —a microfluidic study
M. Nooraiepour, H. Fazeli, R. Miri, H. Hellevang
Published, *Environmental Science and Technology*, 2018, 52(10), 6050-6060

Paper E: Effect of brine-CO_2 fracture flow on velocity and electrical resistivity of naturally fractured tight sandstones
M. Nooraiepour, B. Bohloli, J. Park, G. Sauvin, E. Skurtveit, N.H. Mondol
Published, *Geophysics*, 2018, 83(1), WA37-WA48.

Conference Proceedings

Nooraiepour, M., Park, J., Soldal, M., Mondol, N.H., Hellevang, H. and, Bohloli, B. (2018) Geophysical Monitoring of Gaseous and Supercritical CO_2 Fracture Flow through a Brine-saturated Shale Caprock. *14th International Conference on Greenhouse Gas Control Technologies (GHGT-14)*, 21-25 October 2018, Melbourne, Australia.

Nooraiepour, M., Fazeli, H., Miri, R. and Hellevang, H. (2018) Salt Precipitation during Injection of CO_2 into Saline Aquifers: Lab-on-chip Experiments on Glass and Geomaterial Microfluidic Specimens. *14th International Conference on Greenhouse Gas Control Technologies (GHGT-14)*, 21-25 October 2018, Melbourne, Australia.

Nooraiepour, M., Haile, B.G. and Hellevang, H. (2018) Rock-Physics Characterization and Geomechanical Properties of Mudstones Rich in Siliceous Ooze: A Case Study from the Primary Caprock for Skade Formation, North Sea. *SEG International Exposition and 88th Annual Meeting*, 14-19 October 2018, Anaheim, CA USA.

Nooraiepour, M., Fazeli, H., Miri, R. and Hellevang, H. (2018) Geomaterial Microfluidic Experiment at Reservoir Conditions: Insights on Salt Precipitation in Fractured Shale Caprocks during CO_2 Injection. *InterPore 10th Annual Meeting and Jubilee*, 14-17 May 2018, New Orleans, USA.

Nooraiepour, M. and Mondol, N.H. (2017) Experimental Mechanical Compaction of Reconstituted Mudrocks from the SW Barents Sea: Implication for Exhumation Estimation. *32nd Geological Winter Conference*, 9-11 January 2017, Oslo, Norway.

Nooraiepour, M. and Mondol, N.H. (2016) Petrophysical and Acoustic Properties of Mechanically Compacted Shales – Evaluating Two Barents Sea Top Seal Sequences. *78th EAGE Conference and Exhibition*, 30 May-02 June 2016, Vienna, Austria.

Invited Talks

Nooraiepour, M., Hellevang, H., and Mondol., N.H. (2018) From field-scale to pore-scale: Investigation of caprock properties for CO_2 sequestration. *Energiforskningskonferansen organized by the Research Council of Norway*, May 2018, Oslo.

Nooraiepour, M., Fazeli, H. and Hellevang. H. (2018) Effect of CO_2 phase states and flow rate on salt precipitation in shale caprocks —a HPHT microfluidic study. *Talk delivered at the Final Meeting of the SUCCESS Center*, March 2018, Oslo.

Nooraiepour, M. and Mondol., N.H. (2017) Effect of microstructure and burial on petrophysical properties of mudstones and shales —two case studies. *Talk delivered at the UiO-FirstGeo meeting hosted by FirstGeo Oslo*, December 2017, Oslo.

Nooraiepour, M., Haile, B.G. and Hellevang. H. (2017) Characterization of petrophysical and geomechanical properties Middle Miocene mudstones —the primary caprock for Skade CO_2 storage reservoir. *Talk delivered at the Protect project meeting*, November 2017, Oslo.

Nooraiepour, M., Fazeli, H. and Hellevang. H. (2017) A pore-scale experiment on the salt precipitation during CO_2 leakage from the fractured shale caprocks. *1st national Interpore workshop*, October 2017, Trondheim.

Nooraiepour, M., Fazeli, H. and Hellevang. H. (2016) Fracture flow in organic-rich caprocks: experimental insights. *Talk delivered at the Protect project meeting hosted by the Norwegian Geotechnical Institute*, December 2016, Oslo.

Nooraiepour, M. (2016) Crucial rock properties for sealing CO_2 storage sites. *CLIMIT PhD seminar*, October 2016, Hamar.

Nooraiepour, M. and Mondol., N.H. (2016) Utilizing drill cuttings to characterize source and cap rocks: Barents Sea example. *Talk delivered at the UiO-VNG meeting hosted by VNG Oslo*, October 2016, Oslo.

Nooraiepour, M., Ogebule, O.Y. and Mondol., N.H. (2015) Laboratory compaction of reconstituted mudstones: investigation of petrophysical and acoustic properties. *Talk delivered at the SealCap project meeting*, November 2015, Oslo.

Contents

Part I

Introduction

Chapter 1

Introduction

The present-day anthropogenic emissions of greenhouse gases are the highest ever in Earth history. It is the cause of the observed changes in the climate system that are "unprecedented over decades to millennia" (IPCC, 2014). The observed climate changes, since the 1950s, due to the continued emission of greenhouse gases have had extensive influence on natural systems and human life, and with increasing likelihood will have "severe, pervasive and irreversible impacts for people and ecosystems" (IPCC, 2014). The following chapter briefly introduces the causes, consequences, and proposed solutions for the Earth climate change as a general background for this PhD research. Subsequently, motivations and research objectives for this study are presented, and the dissertation's outline is given.

1.1 Background

The economic and population growth since the industrial revolution have increased anthropogenic greenhouse gas (GHG) emissions (Holloway, 2005; Meinshausen et al., 2009; Riahi et al., 2011). The concentrations of GHGs such as carbon dioxide (CO_2), methane (CH_4) and nitrous oxide (N_2O) in the Earth atmosphere are now higher than ever in the past millennia (Lashof and Ahuja, 1990; Shine et al., 2005). According to the Fifth Assessment Report of the United Nations Intergovernmental Panel on Climate Change (IPCC), it is the collective impact of the anthropogenic increase in GHG concentrations and other anthropogenic forcing that have caused the observed increase in the global average Earth surface temperature. The consequences of global warming and climate change are broad, far-reaching, and long-lasting (IPCC, 2014). It has led to global temperature rise, warming oceans, ocean acidification, glacial retreat, declining Arctic sea ice and Antarctic ice sheets, sea level rise, increased extreme weather and climate events, and changes in terrestrial and marine ecosystems (McCarty, 2001; Root et al., 2003; Riahi et al., 2011). According to the International Energy Agency (IEA), by 2050 the global population will rise from 7 to 9 billion, and over the next 20 years, energy demand is expected to grow by 50 %. While the energy consumption continues to grow, the GHGs emissions, in particular CO_2, have to decline rather fast over the next decades, and near zero emissions of CO_2 and other long-lived GHGs need to be established by the end of the century (IPCC, 2014).

A combination of better energy efficiency, more renewable energy and implementing carbon capture and storage (CCS) is proposed to meet the challenge (IPCC, 2014). Carbon capture and storage (CCS) or carbon capture, utilization, and storage (CCUS) is an essential part of the solution for reducing CO_2 emissions across the energy system in both the 2 °C and the Beyond 2 °C scenarios (IEA, 2016). It provides the time needed to develop the sustainable energy systems for the future while limits the CO_2 emissions from the largest fixed emitters across the world (Holloway, 2005; Gibbins and Chalmers, 2008).

CCS is a technology that involves capturing CO_2 from the large industrial fixed point sources (emitters), transporting the compressed CO_2, and then injecting it into the deep geological formations at a storage site that is carefully selected, where CO_2 is permanently and safely stored (Benson and Cook, 2005; Holloway, 2005; Gibbins and Chalmers, 2008; Leung et al., 2014; Hellevang, 2015). The storage candidates in geological media include deep saline aquifers, depleted hydrocarbon reservoirs, enhanced oil and gas recovery, enhanced coal bed methane recovery, and deep unmineable coal seams (Benson and Cook, 2005). Several researchers have also proposed storage of CO_2 in basaltic rocks (Matter and Kelemen, 2009; Gislason and Oelkers, 2014). For the selection of a geological storage site, three main criteria should be evaluated (Bachu, 2000; Benson and Cook, 2005): (a) storage capacity: the available pore volume in the reservoir rock to accommodate the injected CO_2; (b) injectivity: sufficient permeability of the reservoir rock to allow flow of the injectant; and (c) containment: confinement and sealing capacity of the structure and caprock layers to prevent leakage for a long-term, safe and secure subsurface CO_2 storage. In this research, the primary focus is on containment and properties of sealing caprock sequences. The results, however, are also partly relevant for injectivity assessments.

1.2 Motivation and objectives

The aggregated experiences during the past two decades from the subsurface CO_2 injection at a number of pilot, demonstration, and commercial projects indicate that geological CO_2 storage in deep sedimentary formations is technologically feasible, operationally viable, and environmentally friendly (Holloway, 2005; Michael et al., 2010; Bachu, 2015). To meet the IPCC emission reduction targets, and to make meaningful reductions in the concentration of atmospheric CO_2, millions of tons of supercritical CO_2 ($scCO_2$) have to be injected and stored underground annually (Griffith et al., 2011; Rutqvist, 2012). Ensuring a safe and secure full-scale geologic CO_2 sequestration requires comprehensive analyses of coupled hydrologic–geomechanical–geochemical processes that control fate of the CO_2 plume in subsurface (Rutqvist, 2012). Among other considerations, implementing various monitoring techniques is a necessity for establishing a reliable long-term operation (Wurdemann et al., 2010; Nooraiepour et al., 2018a).

Intrinsic transport properties of a caprock layer govern its ability to prevent fluid flow across a sealing sequence. Fluid flow through the rock matrix, pre-existing and induced fracture networks, and fault systems along with the geomechanical and geochemical factors associated with CO_2 injection defines the sealing capacity and integrity of a caprock layer. Fine-grained argillaceous rocks (e.g., mudstones and shales) and evaporates (e.g., salts and anhydrite) are the commonly identified caprocks for CO_2 storage reservoirs (Michael et al., 2010; Griffith et al., 2011). Because of the markedly distinct pore space characteristics, they are also of fundamental importance as sealing sequences for other anthropogenic-related storage sites such as waste repositories (Mallants et al., 2001; Song and Zhang, 2013). Moreover, fine-grained argillaceous rocks and evaporates have a profound significance for studying geological processes, geoengineering applications, and conventional and unconventional petroleum-related activities.

The overall aim for this PhD study has been to improve the understanding of fine-grained argillaceous caprocks, and to investigate some of the processes that can happen during a potential leakage through the top sealing layers. This dissertation has incorporated multidisciplinary techniques at pore-, core-, and field-scales. It is consist of carefully selected experimental and analytical studies to contribute to the existing knowledge of caprock sequences and to reduce the uncertainties associated with the assessment of containment efficiency for geological CO_2 storage. It also provides answers to some of the less- or uninvestigated questions regarding the CO_2–brine–rock interactions and geophysical monitoring during a potential upward leakage of the CO_2 plume. The present PhD dissertation addresses the following three main research topics:

- **Evolution of mudstones' properties**:

  According to the Wentworth grain size scale (Wentworth, 1922), muds mostly consist of grains smaller than 62.5 µm and comprise silts, clays, and colloids. Muds transform into mudstones as a result of post-depositional processes, namely, mechanical and chemical compactions driven by burial depth, time, and temperature. Mud's constituents derive mainly from weathering, primary production in the receiving basin (Aplin et al., 1999). Burial diagenesis and chemical compaction cause precipitation of siliciclastic and carbonate minerals with minor amounts of sulfides, in addition to the alteration of organic content (Bjørlykke and Høeg, 1997; Aplin and Macquaker, 2011). The broad category of mudstones include a range of rock types with mineralogical composition varying from pure carbonates (e.g., chalk) and siliceous oozes (e.g., diatomites) to siliciclastic mudstones that are composed largely of quartz, feldspars, and clay minerals (Aplin and Macquaker, 2011; Bjørlykke, 2015). Although the term "shale" is commonly used as a catch-all term for fine-grained sediments, it needs to be used with caution as it implies added consolidation, cementation, and particularly fissility (Bjørlykke, 2015). The fissility in shales arises from the preferential alignment of the phyllosilicates that are present in siliciclastic mudstones.

Muds and mudstones are the most common sediment type around the world (Aplin et al., 1999; Schneider et al., 2011). They have the primary control on the fluid flow in sedimentary basins and near-surface environments (Aplin and Macquaker, 2011). Mudstones and shales are of key importance in petroleum exploration and, increasingly more in production (Avseth et al., 2008). Fine-grained organic-rich deposits historically are known as petroleum sources and more recently, in last two decades, as unconventional hydrocarbon reservoirs. The high capillary entry pressure and extremely low matrix permeability make mudstones perfect caprocks and flow barriers in conventional hydrocarbon systems (Schlömer and Krooss, 1997; Hildenbrand and Krooss, 2003; Wollenweber et al., 2010). Such properties are essential for retention of fluid in sedimentary basins and, thus, responsible for the occurrence of overpressure. From a geomechanical perspective, ductile mudstones play a role as planes of weakness along which sediment packages may slide (Rutqvist and Tsang, 2002). Majority of drilling problems happens in mudstone and shale layers, which often are related to pore pressure and hydro-chemical interactions. In near-surface environments, they control natural flow, act as aquitards for water aquifers, and restrict leakage from waste disposal sites (Verma and Pruess, 1988; Aplin et al., 1999; Mallants et al., 2001). They also have broad application in geoengineering and civil engineering projects.

Initial mixture of grain sizes and minerals, and subsequent alterations during mechanical and chemical compactions that transform the deposited mud into a mudstone are determining factors that define physical and chemical properties of mudstones. Unlike chemical compaction and burial diagenesis that are more difficult to replicate in a laboratory, experimental mechanical compaction of brine-saturated samples enables researchers to study the evolution of mudstone properties as a function of effective vertical stress.

The literature on the laboratory compaction of fine-grained clay-rich samples is abundant. For several decades, researchers in different fields have studied changes in rock properties during burial. Firstly, the efforts were focused on changes in total porosity (void ratio) and compaction curves, and then it extended to other properties such as permeability, acoustic velocity, elastic moduli, and anisotropy. Several authors have investigated variations as a function of grain size composition (e.g., Dewhurst et al., 1998, 1999; Yang and Aplin, 2007, 2010; Schneider et al., 2011). A series of laboratory experiments have measured petrophysical properties of synthetic mixtures of clay minerals (e.g., Mesri and Olson, 1971; Al-Tabbaa and Wood, 1987; Vasseur et al. 1995; Mondol et al., 2007). Other researchers looked into the compaction behavior of quartz-clay mixtures (e.g., Knoll and Knight, 1994; Mondol, 2009; Beloborodov et al., 2018). A number of studies have carried out resedimentation experiments (e.g., Seah, 1990; Sheahan, 1991; Santagata and Kang, 2007; Adam et al., 2013). Moreover, intense sampling and testing efforts have been made through the Ocean Drilling Program (ODP) and Integrated Ocean Drilling Program (IODP) to address property variations in the marine mudstones (e.g., Screaton et al., 1990; Saffer et al., 2000; Gamage et al., 2011; Tanikawa et al., 2013; Daigle and Screaton, 2015). The research outcomes show broad range variations that may vary over orders of magnitude. In addition to broad range of variations, there are several inconsistencies among the results of similar experiments on similar material such as compaction of kaolinite clays or quartz-clay mixtures (refer to Paper A and B for further details), which underscores the need for evaluation of validity and reliability of previously published measurements, in addition to study of less-investigated research questions.

Paper A, B, and C are devoted to the experimental mechanical compaction of reconstituted mudstone and shale aggregates, in addition to synthetic mixtures of quartz-kaolinite and quartz-smectite. Variations in physical, hydraulic and acoustic properties as a function of effective vertical stress are studied. The experiments can simulate mechanical compaction of sediments in subsiding sedimentary basins with no superimposed tectonic forces before the onset of chemical compaction and cementation. The laboratory results are compared with well log measurements to further investigate rock physics, geomechanics and compaction-exhumation history of the caprock sequences. Some of the main addressed research questions in this part are: How laboratory compaction of reconstituted and synthetic aggregates can be used to define bounds

and to constrain compaction trends for different properties of mudstones? Is it at all possible, and if yes, how representative it is to use drill cuttings where core samples are not available to reflect the reality of sedimentary basin? How and to what extent does difference in microstructure and composition impact the macroscale properties of mudstone caprocks? What are the distinctive characteristics of mudstones rich in siliceous ooze?
Paper A and B investigate properties of siliciclastic mudstones with implications for caprock sequences in SW Barents Sea. Paper C extended the investigation to an ooze-rich mudstone caprock in the Northern North Sea. Through the concurrent study of naturally-driven aggregates and synthetic binary mixtures, we tried to provide insights into the boundaries, in which mudstones properties may change in the mechanical compaction domain of sedimentary basins. We show how important it is to consider micro-scale characteristics of mudstones when macro-scale properties need to be predicted. These three papers (A, B, and C) also indicate that both compaction trends and depositional trends govern the changes in properties across the basin and even within a given formation.

- **CO_2-induced salt precipitation**:

  The interface between the CO_2 injection wellbore and storage reservoir in near wellbore area may provide maximum CO_2 permeability into the reservoir if injectivity impairment mechanisms can be successfully avoided. The injectivity impairment mechanisms impact porosity and permeability of porous media and can clog fluid transmissivity via physical processes (such as, particle-grain displacement, rock compaction, and shrinkage-swelling) or thermochemical processes (for instance, precipitation of minerals, precipitation of asphaltenes and waxes, and hydrate formation) (Torsæter and Cerasi, 2018). Until recently, most of the scientific studies dealing with injectivity loss in near wellbore area have focused mainly on formation dry-out and salt precipitation because it has the potential to significantly impact the injectivity and even cause complete clogging in the near wellbore area.
  During CO_2 injection, reservoir permeability around the well can be severely reduced as brine pore fluid evaporates into the CO_2 stream and precipitation of salt crystals begin. The permeability loss induces excess pressure build-up and leads to a decline in injectivity during the injection. In the petroleum industry, precipitation of salt crystals is reported in field-scale operations during production from gas reservoirs and storage of natural gas (Place and Smith, 1984; Bette and Heinemann, 1989; Kleinitz et al., 2001; Kleinitz et al., 2003). Moreover, part of the pressure build-up in the Snøhvit and Ketzin CO_2 stor-

age operations is attributed to the salt precipitation (Baumann et al., 2014; Grude et al., 2014). Several micro- to core-scale experimental investigations have also observed and quantified precipitation of halite crystals in the porous medium (Muller et al., 2009; Wang et al., 2009; Oh et al., 2013; Bacci et al., 2013; Kim et al., 2013; Peysson et al., 2014; Roels et al., 2014; Miri et al., 2015; Ott et al., 2015; Tang et al., 2015). Numerical simulations indicated the extent, distribution, and some of the mechanisms related to this phenomenon (Hurter et al., 2007; Giorgis et al., 2007; Pruess and Müller, 2009; Zeidouni et al., 2009; Kim et al., 2012; André et al., 2014; Guyant et al., 2015).

The laboratory flow-through experiments have documented that a moderate reduction in total porosity because of the salt precipitation may have substantial impact on permeability. For instance, 30-86% (Bacci et al., 2013), 50% (Peysson et al., 2014), 60% (Muller et al., 2009), and 75% (Ott et al., 2012) decline in permeability is reported due to halite precipitation in the pore network of Berea sandstone. While it is observed that absolute permeability is decreased (different magnitude for same core sample, though), the published results for relative permeability to CO_2 are contradictory. While Wang et al. (2009) showed approximately 50% reduction in CO_2 relative permeability, Ott et al. (2015) recorded an increase by a factor of five. Such discrepancies between the results of similar experiments are calling for further in-depth investigations and are making application of previous results in real-world cases highly uncertain. Similar discrepancies are abundant for instance in case of injection rate, critical velocity, salt distribution, precipitation location, capillary pressure (Miri and Hellevang, 2016).

Furthermore, it is required to conduct systematic investigations in some other areas. For example, no published research, to our knowledge, provides a systematic study on the effect of CO_2 phase states and thermodynamic conditions on salt precipitation. The inconsistencies regarding the extent, distribution, and significance of halite precipitates, in addition to their influence on the CO_2 phase percolation pathways need to be investigated. While several studies (Ott et al., 2014; Ott et al., 2015; Yin et al., 2016) have shown that salt crystals precipitate only in the brine phase, and therefore, have an insignificant impact on the flow pathways, several other researchers (Verma and Pruess, 1988; Muller et al., 2009; Miri et al., 2015) have indicated that considerable amount of salt crystals can precipitate in the CO_2 phase. As a result, the clogging models based on the latter studies contradict the former and suggest that in the evaporation-precipitation process of salt formation we may face notable variations in the static and dynamic properties of the porous medium.

Design and fabrication of our high-pressure high-temperature (HPHT) microfluidic pressure vessel made it possible to answer a couple of uninvestigated questions and to resolve some of the inconsistencies regarding precipitation of salt crystals in the porous and fractured media. The research questions in paper D are: How do thermodynamic (pressure-temperature) conditions and CO_2 phase states influence extent, distribution and precipitation pattern of salt crystals? What is the collective impact of CO_2 injection flow rate, critical velocity, and thermodynamic conditions on salt precipitation? Is it possible for salt crystals to partially or entirely block potential CO_2 leakage pathways in the caprock? In Paper D, for the first time to our knowledge, we introduced a conceptual framework that suggests salt precipitation is not only a near wellbore phenomenon but also can be a sealing mechanism to impede CO_2 leakage from preexisting fracture networks.

Paper D addresses the physics and dynamics of formation dry-out and salt precipitation on fractured organic-rich shale micromodel. The introduced conceptual model extends the implications from injectivity assessments to CO_2 containment. Conducting lab-on-chip experiments on the Draupne shale as substrate ensures realistic surface energy and wettability characteristics similar to the caprocks for CO_2 storage reservoirs such as the Smeaheia-Northern Light full-scale CCS project. The experiments at HPHT conditions using all three CO_2 phase states (gas, supercritical and liquid) also make the results applicable to the deep subsurface condition. Paper D identifies new governing parameters, and describe several observations that can help build more robust clogging models with proper boundary conditions for modeling salt precipitation in the in the porous and fractured media.

- **Geophysical monitoring of fracture flow**:

  Risk assessment for geological CO_2 storage sites primarily involves with the fast flow leakage pathways that are related to wellbore integrity, fracture networks and fault systems, and leaking eroded or thin caprocks (Nelson et al., 2005; Iding and Ringrose, 2010; Smith et al., 2011). Fracture networks, either natural or engineered, provide major conduits or barriers for fluid flows in different types of porous media. The existence of fractures that affect flow and transport are characteristic of different types of porous media for domains ranging from millimeters to kilometers (Berre et al., 2018). Supercritical CO_2 can migrate out of the geological storage reservoir if the caprock sequences contain a permeable pathway because the buoyancy pressure is usually sufficient enough to exceed the capillary entry pressure for the pathway (Smith et al., 2011). When caprock sequences contain fracture networks, the increased fluid pressure due to CO_2 injection in addition to the buoyancy pressure can create a connecting cluster of open fractures within the network. The secondary permeability associated with the fracture networks and fault systems within the caprocks provide an effective permeability several orders of magnitudes larger than the matrix permeability provided by connected pores.

For geological CO_2 sites with no previous record of hydrocarbon accumulations, there is no guarantee that the caprock layer is free of percolating fracture networks. For depleted oil or gas fields without identified gas chimneys, however, the presence of hydrocarbon accumulations suggests that the caprock does not contain percolating networks or the threshold pressure was high to retain the hydrocarbon column (Smith et al., 2011). On the other hand, production from the hydrocarbon reservoirs or CO_2 injection into the reservoir modify stress states, which may induce new fractures or activate pre-existing closed fractures (Hawkes et al., 2005).

For the low permeability caprocks, where fracture networks and faults systems control the fluid transmissivity, characterization of the potential leaking channels is essential. It includes: (a) the spatial distribution of fractures and faults, (b) orientation and connectivity, (c) permeability, stiffness, and thermo-hydro-mechanical properties, and (d) overall contribution to effective permeability and pressure release (Bildstein et al., 2010; Iding and Ringrose, 2010; Smith et al., 2011). The primary sources of information to construct fracture network models are relevant outcrops, seismic surveys, borehole image logs, in addition to the laboratory core analyses. When geological CO_2 storage is combined with a hydrocarbon production field, production data such as well tests, mud losses, and well logs provide further valuable information. Core-scale experiments and core observations are of great importance because they can bring about firsthand information on the properties of the caprock sequence and thermo-hydro-mechanical characteristics of fractures (Song and Zhang, 2013; Rutqvist, 2015; Sun et al., 2016).

3D seismic surveys are the most widespread technique to monitor and track the CO_2 plume movements within the subsurface (Chadwick et al., 2010; White and Foxall, 2016). It is shown that the variations in P-wave velocity (Vp) reliably determines location of the CO_2 plume because of the reduction in Vp as seismic waves travel through the CO_2-saturated reservoir (Chadwick et al., 2010). Quantifying the CO_2-in-place, however, is more challenging because it requires an accurate relationship between Vp and CO_2 saturation, which it, in turn, depends on fluid distribution in the porous medium in the two-phase brine-CO_2 system (Yamabe et al., 2016). An alternative technique for monitoring storage sites is the electromagnetic survey, which makes use of the strong electrical resistivity contrasts between brine and CO_2 (Falcon-Suarez et al., 2018). It also has the potential to quantify partial CO_2 saturations (Nakatsuka et al., 2010; Falcon-Suarez et al., 2018). The electromagnetic surveys are of much lower resolution compared to the 3D seismic surveys.

Rock physics modeling employs templates for acoustic velocity-CO_2 saturation relationship to map the extent and saturation of the plume. It, however, may introduce some uncertainties because the distribution of brine-CO_2 pore fluids affects the relationship. For instance, the commonly used Biot-Gassmann model (Gassmann, 1951) underestimates partially saturated seismic velocities when we are dealing with patchy fluid mixing. The empirical models (such as Brie et al., 1995), thus, need to be used for matching with the seismic surveys. For providing precise rock physics templates, velocity-saturation relationships can be calibrated and baselined using controlled laboratory experiments for brine-CO_2 fluid displacements. Such templates can then be applied with more confidence to seismic data at the field-scale. Such information is crucial to develop detailed and fit-for-purpose models to robustly track the injected CO_2 and quantify the CO_2-in-place (Chadwick et al., 2010; Würdemann et al., 2010; Falcon-Suarez et al., 2018).

Several laboratory studies have measured geophysical properties of brine- and CO_2-saturated reservoir sandstones (Lei and Xue, 2009; Nakatsuka et al., 2010; Alemu et al., 2013; Chen et al., 2013; Falcon-Suarez et al., 2016). Laboratory measurements have shown that electrical resistivity of porous sandstones is increased to about five times when CO_2 displaced the brine matrix saturation (Nakatsuka et al., 2010; Alemu et al., 2013). Although theoretical models could estimate CO_2 saturation for clean homogeneous rocks, they failed to provide accurate results for heterogeneous shaly core samples (Nakatsuka et al., 2010; Alemu et al., 2013). Variations in total porosity, matrix heterogeneity, and presence of layering relative to flow direction considerably influence the CO_2 distribution pattern during fluid displacement (Lei and Xue, 2009; Alemu et al., 2013; Nakagawa et al., 2013; Falcon-Suarez et al., 2016). Acoustic velocity has shown smaller sensitivity to fluid distribution pattern compared to electrical resistivity (Alemu et al., 2013). During drainage of matrix brine saturation by CO_2, Vp decreased approximately 5-15% (Lei and Xue, 2009; Chen et al., 2013; Falcon-Suarez et al., 2016). Lei and Xue (2009) reported approximately 7.5%, 12%, and 14.5% decrease in Vp for gaseous, liquid, and supercritical CO_2, respectively, when different CO_2 phase states displaced brine matrix saturation.

Despite extensive literature on the geophysical properties of brine- and CO_2-saturated reservoir rocks, there is somewhat limited or no published research on the geophysical responses of brine-CO_2 fracture flow when the matrix flow is negligible. Paper E presents a core-scale experiment in the laboratory, which examines the changes in acoustic velocity and electrical resistivity when CO_2 displaces brine out of the fracture. Paper E also investigates stress dependence, hysteresis, and effect of fluid-rock interaction on fracture permeability. The principal research question was whether it is possible to track CO_2 leakage along a fracture on a core-scale experiment? If yes, what are the sensitivity, detectability, and magnitude of changes in acoustic velocity and electrical resistivity?

Paper E demonstrates that in addition to stress level and pore pressure, mobility and fluid type control the fracture permeability during compression and decompression cycles. The fluid-rock interaction is another factor that affects fracture permeability to the brine-CO_2 system. Paper E investigates which monitoring technique tracks the fluid displacement reliably. The knowledge learned from such core-scale experiment can be useful for monitoring geological CO_2 storage in which primary fluid flow conduit across caprock is the fracture network.

1.3 Outline

This dissertation follows the Manuscript Document Format and is organized in two main parts. The first part is referred to as "Introduction". The introduction to the dissertation provides brief background scientific information for understanding the context and the motivation behind the papers. It also links the papers together and puts the research into a broader context. The introduction part of the dissertation is organized as follows: The current chapter is succeeded by chapter 2, where a brief scientific background is given. Chapter 3 demonstrates the advancement in fabrication and modification of experimental setups and laboratory techniques during this PhD research. Chapter 4 summarizes the motivation and objectives, methods and procedures, and main results from the papers. The last chapter of the introduction (chapter 5) presents the conclusion and some suggestions for further research.

The second part of the dissertation consists of the published articles and submitted manuscripts. The results of the PhD research have contributed to scientific knowledge via five manuscripts (from now on referred to as "Paper"), where I am the first author in all of them. The extended abstracts and conference proceedings are enclosed at the end of the dissertation in the appendix in chronological order.

Chapter 2

Scientific Background

In this chapter, the contextual information that are important to understand the papers are briefly presented. First, I will provide technical background about the fine-grained caprock sequences, and the importance of containment criterion in CCS projects. The caprock sealing mechanisms and seal potential are then discussed.

2.1 Evolution of rock properties

Figure 2.1 shows a schematic representation of sandstone and mudstone compaction trends during burial. The initial porosity at the time of deposition for sands and muds are approximately 40 % and 80 %, respectively (Zimmer et al., 2007; Day-Stirrat et al., 2010; Koochak Zadeh et al., 2016; Nooraiepour et al., 2017b). A relatively shallow crossover, however, between sandstone and mudstone compaction curves is expected because constituents of the mudstones are more prone to compaction than the coarser sand-sized grains in sandstones (Avseth et al., 2003; Bjørlykke, 2015). The siliciclastic deposits, muds and sands, transform to mudstones and sandstones through mechanical and chemical compactions during burial. With the added consolidation, cementation, and fissility due to higher temperatures and pressures, the fine-grained argillaceous rocks transform to shales (Aplin and Macquaker, 2011). During burial, as a result of mechanical and chemical compactions, siliciclastic sediments undergo both physical and mineralogical changes (De Segonzac, 1970; Hower et al., 1976; Chilingarian et al., 1995; Vasseur et al., 1995; Bjørlykke, 1998; Dewhurst et al., 1998; Nadeau et al., 2002; Mondol et al., 2007; Thyberg et al., 2010; Nooraiepour et al., 2017b).

The conceptual model presented in Figure 2.1 demonstrates the reduction of initial porosity associated with mechanical processes in addition to the concurrent and subsequent chemical diagenetic reactions. The interplay of mechanical and chemical compaction impacts petrophysical and geomechanical properties such as total

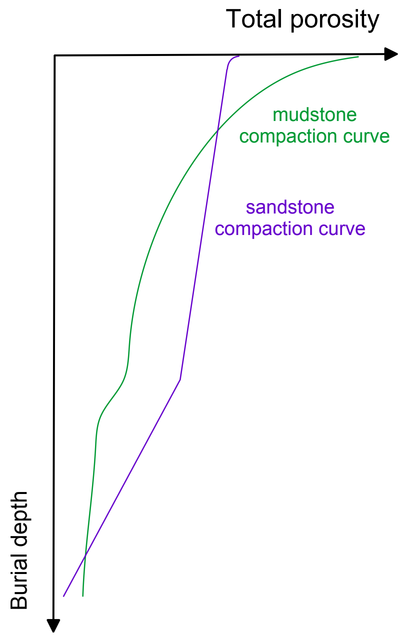

Figure 2.1: Generalized compaction curves for mudstones and sandstones during mechanical and chemical compactions (modified after Avseth et al., 2003 and Bjørlykke, 2015).

porosity, bulk density, permeability, acoustic velocity, elastic moduli, and strength of the sediments.

In the mechanical compaction domain, effective stress (σ_e) causes the decrease in total porosity and the increase in bulk density of sediments. The effective stress (σ_e) is the difference between the overburden load of sediments (σ_v) and fluid pore pressure (P_p). The volume change and consequent reduction in porosity in the mechanical compaction domain are associated with rearrangement, reorientation, and even breakage of the grains (Chuhan et al., 2003; Fawad et al., 2010). While during shallow and intermediate burial effective stress governs the changes in physical and acoustic properties, cementation of biogenic carbonate or silica (Opal-A to Opal-CT) may also cause lithification at shallow depth levels (Bjørlykke, 2015). At higher temperatures in the deeper part of the basin, chemical compaction begins as a result of clay mineral transformation and precipitation of pore-filling micro-quartz cement (Bjørlykke, 1998; Thyberg and Jahren, 2011; Goulty et al., 2016). The temperature, time, and surface area for growth control the kinetics and the thermodynamics of the chemical compaction (Bjørlykke and Aagaard, 1992). At temperatures around 65-70 °C, provided that the potassium source is available, transformation of smectite to illite starts (Hower et al., 1976; Bjørlykke, 1998). It is the most important clay diagenetic transformation in mudstones and shales before 120 °C (Goulty et al., 2016). The geochemical reaction of smectite to illite transformation releases water, silica, and cations, which can further react with calcite and kaolinite and form ankerite and chlorite (Cuadros and Linares, 1996; van de Kamp, 2008). Moreover, Milliken and Day-Stirrat (2013) also showed majority of detrital plagioclase might get albitized because of the reaction with the sodium ions released from smectite to illite transformation. Other geochemical reactions and diagenetic changes in the temperature ranges between 70 °C and 120 °C are presented by many authors (such as, De Segonzac, 1970; Hower et al., 1976; Freed and Peacor, 1989; Bjørlykke, 1998; and Nadeau et al., 2002). Above 120 °C, kaolinite and K-feldspar start to transform to illite clay minerals supplying further silica for quartz cementation (Chermak and Rimstidt, 1990; Giorgetti et al., 2000).

There are two different conceptual models, as presented in Figure 2.2, which explain the post-depositional changes in mudstones. These two frameworks define the relative impact and the domain of influence for mechanical and chemical compactions as a function of temperature or burial depth. First conceptual model, the left side of Figure 2.2, states that after the initial mechanical compaction, there is a transition zone during which clay diagenesis, cementation, and chemical compaction begin while mechanical compaction is still active (Bjørlykke and Høeg, 1997; Bjørlykke, 1998). At higher temperatures, chemical compaction is the only governing mechanism that continues, by implication, independent of the effective stress (Bjørlykke and Høeg, 1997; Bjørlykke, 1998). The importance, presence, and span of the transition zone is, however, discussed and highlighted dissimilar in literatures about

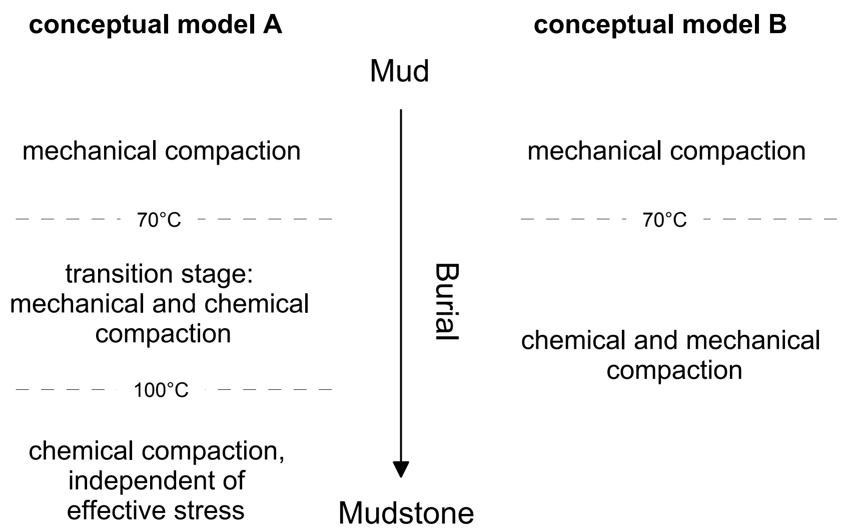

Figure 2.2: Alternative conceptual models for the relative impact of mechanical and chemical compactions on mudstones during burial (modified after Goulty et al., 2016).

the first model (e.g., Bjørlykke, 2015). For instance, Storvoll and Brevik (2008) assert that at the onset of chemical compaction when quartz cement precipitates, the grain contacts becomes more stable, the stress distributes on a larger surface areas because of the cement, and as a result increase in effective vertical stress becomes insufficient to overcome the strength and stability of the grain framework. They, thus, conclude that it marks the end and stop of mechanical compaction and the beginning of sole chemical compaction (Storvoll and Brevik, 2008).

The right side of Figure 2.2 presents the second conceptual model. It states that both chemical and mechanical compactions are responsible for the changes in mudstone properties after the onset of clay mineral transformation (Dutta, 2002; Lahann, 2004). Moreover, in the second model, there is no implication about mechanical compaction getting negligible at temperatures above 100 °C. Goulty et al. (2016) documented evidence of mechanical compaction in response to increased effective stress up to 130 °C. Another group of scientists, such as Day-Stirrat et al. (2010), while using the first conceptual model, have incorporated the second model by stating that there is the mutual impact of mechanical and chemical compactions at deeper depths. Chemical compaction dominates the mutual impact, and the effect of mechanical compaction eventually fades away (Day-Stirrat et al., 2010; Milliken and Day-Stirrat, 2013). In which depth or above which temperature interval, the mechanical compaction fades away and the chemical compaction becomes the only governing factor, however, remain elusive.

In contrast to what Figure 2.1 illustrates for mudstone compaction trend, fine-grained argillaceous rocks show a considerable scatter in compaction curves during burial, even in the mechanical compaction domain (Chilingarian et al., 1995; Giles et al., 1998; Mondol et al., 2007; Avseth et al., 2010; Bachrach, 2016; Nooraiepour et al., 2017b). Depending on the microstructure and composition of the constituents in terms of mineralogy and grain size, a bound should be used to describe mudstone properties instead of a single line or equation.

For instance, Figure 2.3 indicates the total porosity–effective vertical stress, vertical permeability–effective vertical stress, and vertical permeability–total porosity relationships for synthetic binary quartz-clay mixtures. It shows how these properties and trend lines vary with respect to endmember mineralogical composition and grain size distribution. In Figure 2.3, the most abundant constituents of mudstones are used to demonstrate the range of potential variations until 25 MPa effective vertical stress, which corresponds to 2-2.5 km burial depth in normally compacted basins. At 25 MPa effective vertical stress, the laboratory compacted specimens show the following range of final porosity presented in descending order in mixtures of smectite-rich: 29-42%, pure silt-sized quartz: 34 %, and kaolinite-rich: 19-29%. There are 23 % variations in final total porosity of synthetic mudstones and approx-

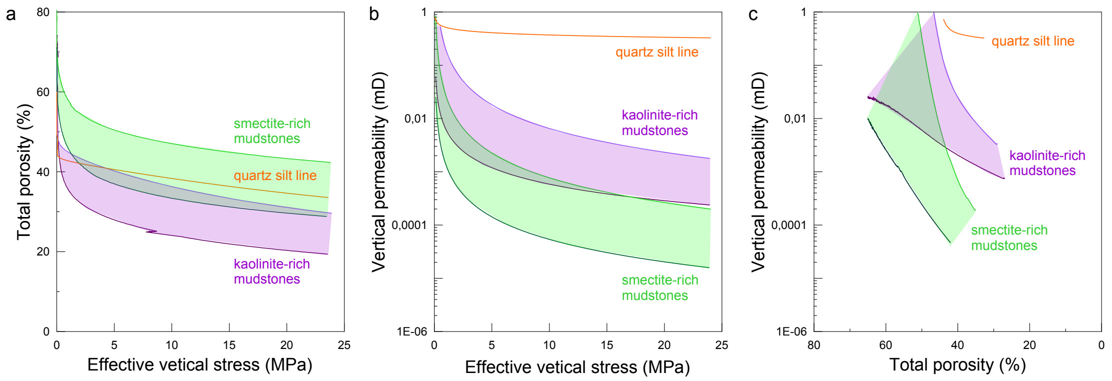

Figure 2.3: Variation of total porosity and vertical permeability as a function of effective vertical stress during mechanical compaction for different mixtures of quartz-kaolinite and quartz-smectite synthetic binary mudstones. The presented laboratory compaction curves are produced in this PhD research.

imately five orders of magnitude difference in vertical permeability at the end of the mechanical compaction domain (Fig. 2.3a, b). Nooraiepour et al. (2017b) have reported that reconstituted mudstone and shale aggregates may even show total porosity of 10 % at 25 MPa effective vertical stress. This broad range of variation indicates how important it is to incorporate micro-scale properties into the geological and geophysical interpretations through rock physics understanding.

Until recently, though, mudstones and shales have often been considered as a unique type of lithology, and not much attention has been given to the micro-scale properties (Avseth et al., 2008). The mechanical properties and elastic moduli are also increasing as a result of increasing effective vertical stress, which in turn leads to an increase in acoustic velocity during burial (Avseth et al., 2005; Nooraiepour et al., 2017a). The elastic moduli increase rapidly during early compaction, up until 10 MPa, because of the significant porosity loss at low-stress levels. Afterward, they show a steady and gentle increase as the grains get closer and become more densely packed. While during mechanical compaction these moduli increase monotonically with the decrease in porosity or increase of vertical effective stress, they show different behaviors when chemical compaction begins (Storvoll and Brevik, 2008; Nooraiepour et al., 2017b). In particular, shear modulus reacts distinctly above and below an apparent knee-point, which represents the initiation of quartz cementation (Storvoll and Brevik, 2008; Baig et al., 2016). The knee-point is characterized by a sharp increase in shear modulus and change in the trend line.

In the mechanical compaction domain, the Athy-like exponential decline in porosity can generally describe porosity compaction curves (Athy, 1930). The shape of the compaction curves is controlled by microstructure (Velde, 1996; Schneider et al., 2011), which in turn, determines the pore space properties and the available intergranular volume for cementation (Milliken and Day-Stirrat, 2013). At the onset of chemical compaction, the precipitated cement does not influence porosity or bulk density greatly because the pore volume only changes slightly (Marcussen et al., 2010). It, however, results in a significant increase in velocity-depth trends (Vernik and Nur, 1992) as incipient quartz cementation near grain contacts causes a rapid and significant framework stiffening (Winkler, 1983; Bernabé et al., 1992; Avseth et al., 2010). The early quartz cementation, therefore, causes a substantial increase in shear modulus. It is why shear wave velocity indicates much higher sensitivity to weak cementation compared to compressional wave velocity (Han and Batzle, 2006; Storvoll and Brevik, 2008). As burial depth increases and chemical compaction continues, total porosity decreases and acoustic velocity increases. However, it has less impact on the continued stiffening of grain framework, and consequently elastic moduli (Vernik and Nur, 1992; Storvoll et al., 2005).

Rock properties of the fine-grained argillaceous sediments are strongly affected by local geologic trends and may markedly change even within a sedimentary basin (Avseth et al., 2003; Loseth et al., 2011; Nooraiepour et al., 2017b). The geological trends can be divided into two categories: compaction trends and depositional trends (Avseth et al., 2003; Haile et al., 2018). In other words, critical geologic parameters that determine the evolution of rock properties are either related to burial history or depositional environment. How post-depositional processes modify mudstone properties during burial through mechanical and chemical compactions are presented above. How depositional trends and lateral variability dictate the changes in macro-scale rock properties should also be incorporated in basin-wide interpretations. Such knowledge and understanding is crucial particularly in the areas with little or no well log information to constrain geological and geophysical models and to reduce uncertainties in the prediction of rock and fluid properties (Avseth et al., 2003).

2.2 Containment

For CO_2 sequestration in geological formations, a porous and permeable reservoir rock such as sandstone is required to bring about the necessary storage capacity and injectivity (Hellevang, 2015). Under the subsurface thermodynamic (pressure-temperature) conditions relevant to the majority of the storage candidates, CO_2 is in the supercritical state with a fluid density of 30-40% less than the surrounding brine or pore water (Bachu, 2015; Miri and Hellevang, 2016). Because of the buoyancy, thus, the CO_2 plume tends to move upward. The reservoir rock should be overlain and confined by an impermeable layer to impede movements of buoyant

CO_2, displaced brine and other mobilized fluids ensuring that they do not leak into the overlaying sequences, lateral structures, and sensitive environmental or economic resources (Bachu, 2000; Shukla et al., 2010; Song and Zhang, 2013). It is called the seal or caprock layer – a critical component of geological CO_2 storage. The caprock for CO_2 storage reservoirs are often fine-grained argillaceous rocks and evaporates (Michael et al., 2010; Griffith et al., 2011). These rocks are also the typical caprocks for the hydrocarbon reservoirs, waste repositories, as well as natural CO_2, N_2, and He resources.

A safe underground CO_2 injection and the storage security are primarily influenced by caprock integrity, particularly during and in the early phases after the injection (Griffith et al., 2011). To evaluate caprock integrity, it is important to identify various cases and scenarios for a potential CO_2 leakage and migration from the storage reservoir. Figure 2.4 presents several mechanisms for such potential leakage (Benson and Cook, 2005; Song and Zhang, 2013). These leakage mechanisms include (a) CO_2 leakage due to poorly completed injection well up the wellbore and into the shallower horizons; (b) CO_2 leakage via poorly plugged abandoned well up the wellbore and into the shallower horizons; (c) leakage into seal matrix when CO_2 pressures exceed the capillary entry pressure of the seal; (d) CO_2 escape through thin laterally discontinuous eroded caprock; (e) CO_2 migration via a permeable pre-existing fault or induced fracture system; and (f) hydrodynamic flow of plume or the dissolved CO_2 out of the closure.

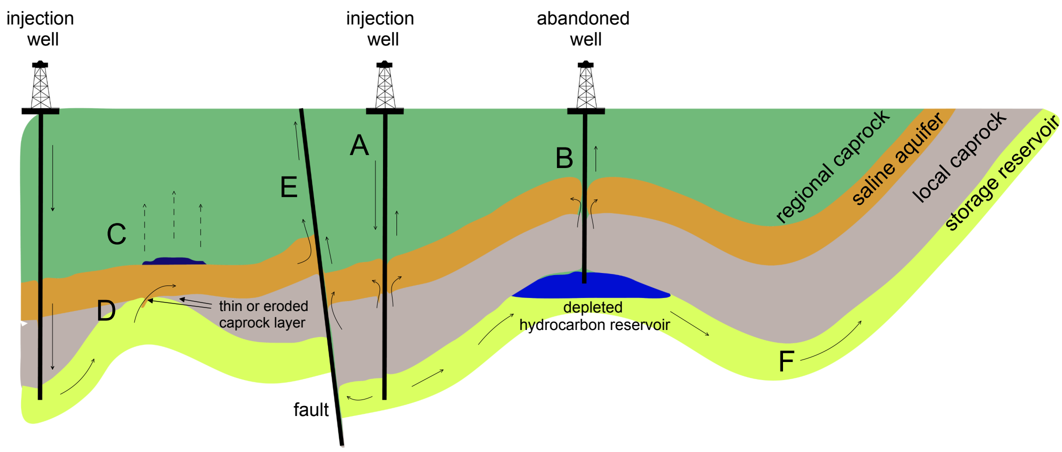

Figure 2.4: Potential leakage mechanisms during subsurface CO_2 storage. A: leakage through poorly completed injection well; B: leakage through poorly abandoned well; C: capillary break-through; D: leakage through thin or eroded caprock; E: leakage through the fault and fracture system; F: hydrodynamic flow out of the closure (modified after Benson and Cook, 2005).

Another mechanism is the CO_2 molecular diffusion into the caprock. The effective penetration rate and length, however, via the CO_2 molecular diffusion is somewhat limited in time scales of less than thousands of years (Song and Zhang, 2013; Jacops et al., 2017).

In petroleum exploration, both in basin-wide investigation of hydrocarbon systems and field-scale prospect identification, it is essential to determine which caprock layer has the potential for trapping economic volumes of hydrocarbon accumulations (Downey, 1984; Schlömer and Krooss, 1997; Cartwright et al., 2007). Multiple parameters such as lithology, pore space characteristics, thickness, ductility, and fracture density influence the caprock properties (Schlömer and Krooss, 1997; Rutqvist and Tsang, 2002; Hildenbrand and Krooss, 2003; Wollenweber et al., 2010; Song and Zhang, 2013; Nooraiepour et al., 2017a). A range of microscopic to macroscopic investigations, therefore, is required to analyze the seal properties. Similar to the petroleum industry, determining the viability of caprock sequences for secure long-term retention of large volumes of the injected CO_2 is a crucial prerequisite in the storage site selection (Halland et al., 2011; Rutqvist, 2012; Bohloli et al., 2014).

When we evaluate the leakage risk, or containment probability, lithological properties of the caprock should be taken into account to determine its sealing capacity (Kivior et al., 2002; Ghanizadeh et al., 2013; Song and Zhang, 2013). The seal capacity is the volume of CO_2 that the caprock can withhold because of the capillary forces (Watts, 1987; Amann-Hildenbrand et al., 2013). Moreover, the lower boundary of the caprock is in contact with CO_2-saturated brine pore fluid, which can cause geochemical interactions of CO_2–brine–rock and consequent changes in rock properties (Alemu et al., 2011; Liu et al., 2012). The knowledge of mineralogical composition, the chemistry of formation water, and CO_2 properties is necessary to gauge the geochemical properties and to predict the potential reactions (Alemu et al., 2011; Liu et al., 2012; Hellevang, 2015). The geomechanical analyses indicate the integrity and potential mechanical responses of the caprock layer as a response to the stresses and perturbations induced by CO_2 injection and subsequent relaxation (Rutqvist and Tsang, 2002; Bohloli et al., 2014; Jeanne et al., 2016).

In addition to the geomechanical properties and changes in stress state, it is critical to consider potential deterioration in mechanical strength caused by interaction with reactive CO_2-rich pore fluids for the overall evaluation of CO_2 containment (Gaus, 2010; Liu et al., 2012). The sealing integrity of the caprocks may also be affected by faults, fractures and microfractures, which might be preexisting or induced and enhanced by changes in pressure due to CO_2 injection (Rutqvist et al., 2007; Griffith et al., 2011; Song and Zhang, 2013). The magnitude of the change in pressure is controlled by the permeability, location of the injection well, and whether the system is closed or open to discharge and displacement of brine (Rutqvist et al., 2007; Griffith et al., 2011). In addition to individual mechanisms, coupled hydrologic–thermal–geomechanical–geochemical processes may increase or decrease the permeability of leaking channels and bypass conduits due to dissolution or mineral precipitation, respectively.

2.3 Seal potential

Majority of the works on caprocks have focused on their role as sealing sequences for hydrocarbon systems (Downey, 1984; Watts, 1987; Schlömer and Krooss, 1997; Cartwright et al., 2007; Hantschel and Kauerauf, 2009; Aplin and Macquaker, 2011). Most of the published research primarily consider only the hydrocarbon column height retention of the caprock layers. The primary sealing mechanism for the caprocks is the capillary sealing, which takes place at the reservoir–caprock interface (Watts, 1987; Amann-Hildenbrand et al., 2013). It counteracts the buoyant forces with capillary forces. For a caprock layer to be effective in both CO_2 storage and hydrocarbon systems, though, several other parameters are essential such as lateral continuity over the extent of the storage reservoir, sufficient thickness, stratigraphic homogeneity, and lack of open fracture and fault networks (Vavra et al., 1992; Griffith et al., 2011; Song and Zhang, 2013). To evaluate seal potential, as defined by Kaldi and Atkinson (1997), three parameters should be investigated: (a) seal capacity: the column height of CO_2 (or hydrocarbons) supported by the capillary properties of the caprock; (b) seal geometry: the structural position, lateral continuity (areal extent) and thickness of the caprock; and (c) seal integrity: the geomechanical profile of the caprock, and the tendency to brittle failure or ductile behavior. The seal potential is often evaluated on a storage site by storage site basis or structure by structure (Hantschel and Kauerauf, 2009; Michael et al., 2009). Kivior et al. (2002) proposed the following relationship to evaluate and compare seal potential (SP) for different caprocks:

$$SP = (\frac{SC}{VSC}) \cdot (\frac{AES}{AEC}) \cdot (\frac{ST}{FT}) \cdot (1 - SI)$$

where SP is seal potential; SC is seal capacity; VSC is vertical structural closure; AES is areal extent of the seal; AEC is structural or stratigraphic closure; ST is seal thickness; FT is potential fault throw in caprock; and the SI is seal integrity parameter. To compare the seal potential of caprocks at different storage candidates, semi-quantitative values can be assigned to each parameter. In addition to storage capacity and injectivity criteria, the seal potential value can represent the containment criterion to make an overall assessment of CO_2 storage sites.

The seal capacity (SC) addresses the CO_2 column height that can be retained by the capillary forces of the caprock (Watts, 1987; Amann-Hildenbrand et al., 2013). It acts against the upward buoyant forces that the CO_2 plume exerts on the caprock, and prevents CO_2 migration into and through the matrix of the caprock. The ability of the caprock to prevent CO_2 plume upward movement through the capillary sealing mechanism is controlled by the diameter of the interconnected pore throats, the relative density of CO_2-brine fluid phases, and petrophysical properties such as wettability and interfacial tension (IFT) of the CO_2-brine–rock system (Wollenweber et al., 2010; Amann-Hildenbrand et al., 2013; Bennion and Bachu, 2013; Song and Zhang, 2013). According to Watts (1987), caprocks controlled by the capillary sealing mechanism are referred to as membrane seals. For a membrane seal, the difference between the wetting phase (brine pore fluid) and non-wetting phase (CO_2 or hydrocarbon) defines the capillary pressure, and the surface free energy determines the mineral surface wettability (Teige et al., 2010). At the reservoir–caprock interface, there is a dramatic change in permeability and pore space characteristics of reservoir and seal sequence. The buoyant fluid in the pore volume of the reservoir rock, hence, will be trapped under the caprock until the capillary entry pressure is exceeded. When the pressure passes the capillary entry pressure, CO_2 begins to enter matrix of the caprock and continues to migrate upward. The containment, however, is not lost until the leaking CO_2 has migrated past through the caprock layer (Heath et al., 2012; Song and Zhang, 2013).

The seal geometry considers thickness, lateral continuity and structural position of the caprock (Kaldi and Atkinson, 1997; Kivior et al., 2002). Only when the caprock layer overlies the reservoir and covers the storage structure, the membrane sealing mechanism actively preserve the CO_2 plume. From a theoretical perspective, even very thin caprocks provide membrane sealing, and thus, seal capacity (Watts, 1987). A thick caprock, however, is more favorable as it brings about better sealing characteristics if capillary breakthrough occurs. Thick caprocks provide a thicker permeable barrier, delay the breakthrough time, and diminish the leakage rate (Amann-Hildenbrand et al., 2013; Ghanizadeh et al., 2013). Moreover, the probability of having sub-seismic through-going fracture and fault system decreases as thickness increases.

The seal integrity (SI) includes geomechanical properties of the caprock such as brittleness–ductility, compressibility, elasticity (Kaldi and Atkinson, 1997; Song and Zhang, 2013). It also deals with the leakage through faults or fracture networks, and the probability of creating new fractures and reactivating previously existing faults (Rutqvist and Tsang, 2002; White and Foxall, 2016). Parameters such as mineralogical composition, lithology, state of overburden and pore pressure, regional stresses, pre-existing planes of weakness, and magnitude and orientation of thermal-and pressure-induced stresses affect integrity of the caprock layers (Bennion and Bachu, 2005; Rutqvist et al., 2007; Griffith et al., 2011; Song and Zhang, 2013; White and Foxall, 2016; Nooraiepour et al., 2017a). Changes in the stress regimes during subsurface CO_2 injection may result in the compaction and dilatation of the reservoir and caprock units, and cause mechanical failure due to injection or relaxation (Rutqvist and Tsang, 2002).

Chapter 3

Advancement in Laboratory Techniques

This dissertation includes several laboratory investigations, during which I had to design fit-for-purpose experiments to perform systematic studies and to answer some open or less-investigated questions. It was necessary, thus, to modify and tailor-make the available experimental setups at the Department of Geosciences of the University of Oslo (UiO) and at the Norwegian Geotechnical Institute (NGI). A high-stress oedometer cell equipped with acoustic measurement transducers, simultaneous fluid flow and geophysical monitoring laboratory setup, and a core flooding system were used in this PhD study. Moreover, I was part of a team of two, who designed and fabricated a microfluidic pressure vessel to house geomaterial micromodel specimens. This chapter introduces the developed pressure vessel and fabrication technique for making microfluidic specimens.

3.1 Description of experimental apparatus

For decades, lab-on-chip experiments and micromodels have provided researchers in various research areas the opportunity to observe fluid flow and solute transport within the pore space (Karadimitriou and Hassanizadeh, 2012). However, majority of the microfluidic studies use engineered material, simple geometries, and ambient pressure-temperature conditions, which makes relevance and applicability of their results limited in the context of deep subsurface conditions in CCS and petroleum sectors (Porter et al., 2015; Nooraiepour et al., 2018b). In CCS, particularly, CO_2 is injected underground in supercritical state, which implies elevated pressure and temperature conditions. Moreover, $scCO_2$ shows remarkably different properties compared to gaseous and liquid phase states (Ji et al., 2005; Bennion and Bachu, 2008; Miri et al., 2014). We, therefore, designed and manufactured a novel stainless steel pressure vessel to accommodate experimental micromodels. For the high-pressure high-temperature (HPHT) microfluidic experiments, we have developed a technique for fabrication of specimens that can make use of a variety of substrate materials. For instance, the micromodel specimens can be made of natural and synthetic materials, such as natural rocks, mineral chips, concrete, cement, ceramics, and glass. Figure 3.1 shows a schematic of the custom-designed pressure vessel, where the top view and cross-section of the microfluidic vessel are demonstrated.

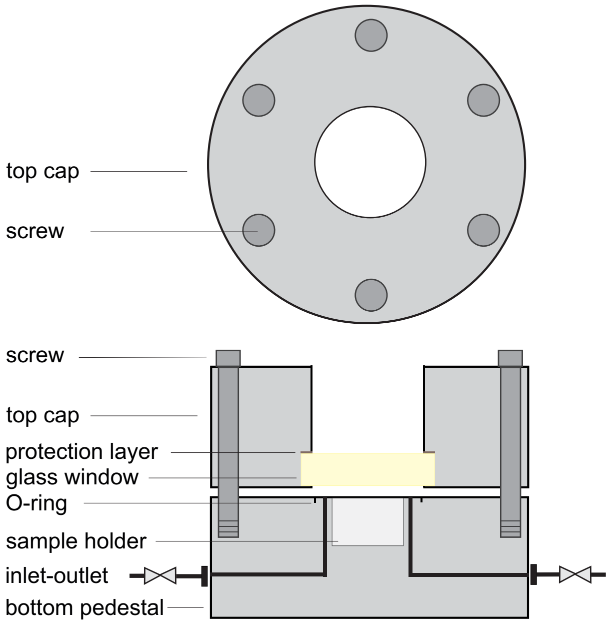

Figure 3.1: Schematic of the HPHT microfluidic pressure vessel.

As shown in Figure 3.1, the experimental pressure vessel consists of two compartments, the top cap and the bottom pedestal. The top cap houses the monitoring glass window, seals the sample holder, and covers the pressure vessel inner part. Moreover, an O-ring seals the circumference of the sample holder and keeps the injected fluid within the chamber of the pressure cell. In this way, the pressure vessel is completely sealed even at high fluid pressures. The sample holder is located in the bottom pedestal (Fig. 3.1). The bottom pedestal connects the microfluidic specimen within the sample holder to the fluid inlet and outlet. The height of the microfluidic specimens is designed to be approximately 500-1000 μm higher than the depth of the sample holder. The considered measure for the specimen height ensures proper contact between the specimen's top and the viewing glass. Six long screws (60° intervals) were also incorporated to seal the pressure vessel and to connect the top and bottom compartments (Fig. 3.1). The screws can be tightened enough to press the glass window on the specimen's top and the surrounding O-ring. It assures active stress between the sealing surface and the specimen. We have tested the microfluidic vessel for high pressure-temperature conditions, and it showed a safe working capacity up to 20 MPa fluid pressure and 80 °C temperature.

The microfluidic pressure vessel was then placed and connected to an AFS 200 core flooding system (Core Laboratories). Figure 3.2 illustrates a schematic of the experimental setup. The microfluidic pressure vessel was put under a stereo microscope within an insulated forced-convection air bath to ensure an equilibrated and steady temperature within the experimental setup. The fluid injection system consists of one dual-cylinder syringe pump (Teledyne Isco, 100DM). A back pressure regulator and a single-cylinder syringe pump (Teledyne Isco, 500D) control the fluid pressure inside the system. Two pressure transducers measure fluid pressure at the inlet and outlet of the microfluidic pressure vessel. To equilibrate brine and CO_2 phases and accumulate experimental fluids, two stainless steel fluid transfer vessel were accommodated within the forced-convection air bath (Fig. 3.2). The effluent fluid may pass through a two-phase separator, where the liquid outlet can be measured by either the built-in separator or a mounted high-precision digital scale. Three gas mass flow controllers, at three different working ranges, detect and measure the gas outflow after the back pressure regulator. For the plumbing of the hydraulic connections, we used high-pressure steel tubing, fittings, and valves. To visualize and digitally record the experiments, we used a Nikon SMZ stereo microscope (visible light) (Fig. 3.2).

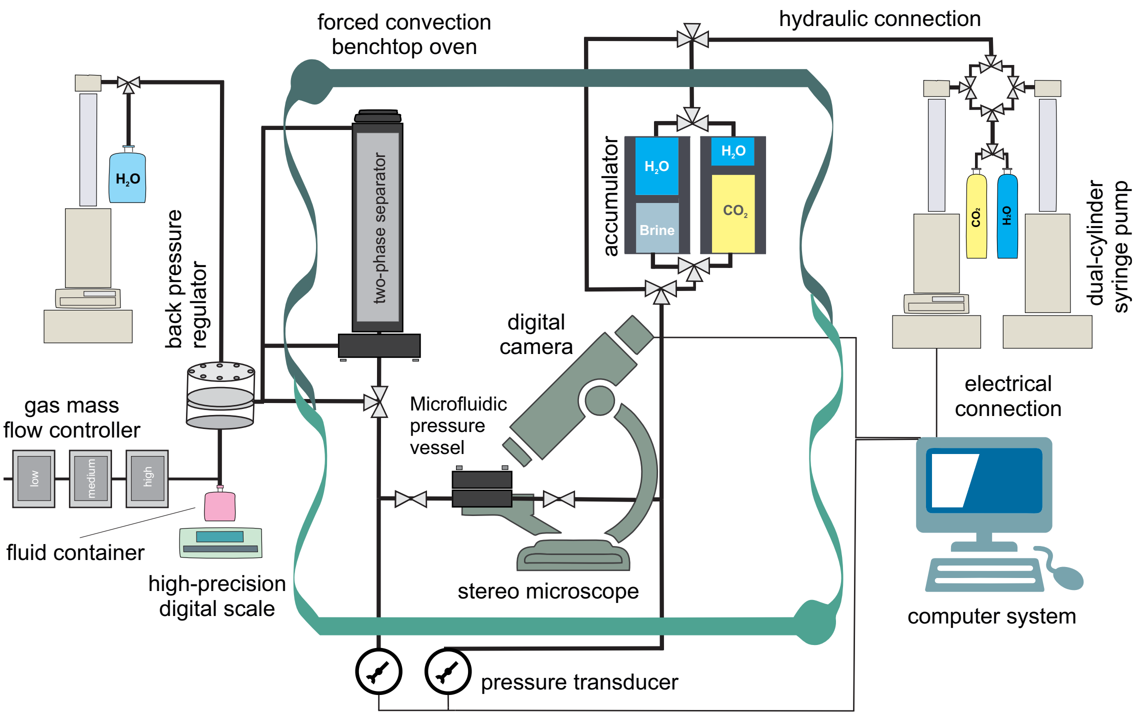

Figure 3.2: Schematic of the experimental setup used in lab-on-chip reactive transport experiments.

The Nikon SMZ is a Greenough-type stereo microscope, which makes use of two separate optical paths and an angular offset to generate a three-dimensional image. We equipped the trinocular head of the microscope with a digital camera to record a stream of high-resolution live video at 30 frames per second through the ScopeView 3.0 software. The recordings are conducted from the top view through the glass window with bright field condition.

3.2 Fabrication of microfluidic specimens

To prepare samples for fabrication of microfluidic specimens, we cut the samples in less than 2.5 cm diameter sizes. Before putting the samples inside the epoxy resin, they are dried at 40 °C for three days to minimize the brine saturation within the samples. We chose to fabricate the specimens using the cold mounting procedure to limit the potential alterations of the rock substrates. In the designed cold mounting procedure, the dried samples are placed inside a 25 mm wide and 15 mm high cylindrical plastic mold, and then the mold is filled with the epoxy resin. The brittle, friable, and porous materials can be vacuumed before adding the epoxy, or the samples can be impregnated with epoxy under vacuum. To let the mold harden, it was left overnight. Afterward, several automatic grinding and polishing steps are being performed to (a) reach the surface of the rock substrate and remove the overlying epoxy, and (b) provide a flat unscratched surface for etching the pore network or fracture patterns. During the experiments, the injected fluid will be partly in contact with the epoxy nearby the inlet and the outlet. However, the cold mounting procedure does not alter properties of the rock substrate. The epoxy plays a role as a non-reactive phase, and no interaction between the epoxy and injectant is expected.

When we complete fabrication of the microfluidic specimens, we use laser-scribing technique to etch the desired pore and fracture network on the surface of the microfluidic substrate. To scribe the designed pattern, we use a Rofin scribing laser at the microsystems and nanotechnology laboratory (MiNaLab) at the University of Oslo. It is an air-cooled solid-state laser cutter with the continuous-wave operation and Q-switch assembly that provides high performance and precision pulses. A CombiLine workstation houses the PowerLine E Air 25 laser maker and provides integrated computer control and programmable z-axis positioning of the marking head. The CombiLine system (Rofin) is equipped with visual laser marker software, which allows direct transmission of required marking data from computer to the laser marker. The fracture network is scribed using a 532 nm scribing laser at 25A, 15000 Hz and 200 mm/s. The scribing is performed twice with an interval time of 5 minutes between each execution to keep the sample heating to a minimum. Moreover, a high scanning speed, high power, and low frequency were selected to maximize ablation, minimize heating of the sample, and limit the heat affected zone. Subsequently, the ablated debris and heat affected material are cleaned to reach the undisturbed surface of the substrate. To remove the ablated debris, we use micro-scratcher blades under an optical microscope. Surface profilometry is then performed to capture geometry and dimensions of the eventual pore and fracture network patterns before the experiments.

We are making use of the HPHT microfluidic pressure vessel for a variety of research purposes. The first publication using the developed experimental setup and laboratory technique for sample preparation was on the physics of salt precipitation (Nooraiepour et al., 2018b). The second manuscript is in the final stage of preparation on the effect of mineral heterogeneity on geometry evolution and mineral dissolution in fractured carbonate-rich caprocks. The third manuscript is also under preparation on the nucleation and mineral growth of smectite clay minerals.

Chapter 4

Summary of Papers

This PhD dissertation comprise five papers. Here, a summary of each paper including the motivation and objectives, methods and procedures, and main results are presented. In part II of the dissertation, the papers in the following order are listed. The dissertation addresses the following three research topics:

4.1 Evolution of mudstones' properties (Paper A, B, and C)

Paper A: *Experimental mechanical compaction of reconstituted shale and mudstone aggregates: Investigation of petrophysical and acoustic properties of SW Barents Sea cap rock sequences*

Motivation and objectives

In this paper capability of the reconstituted mudstone and shale aggregates to reflect reality of sedimentary basins in the laboratory is evaluated. There is a wide variety of studies that introduce compaction trends and empirical equations to describe variations in properties of mudstones and shales during burial based on synthetic binary mixtures. The fine-grained clastic sediments in nature, however, comprise a complex multi mineral composite, which may undergo different compaction than synthetic materials with various proportions of clay and quartz. Moreover, we were interested to see whether it is possible, and how representative it is to use drill cuttings where core samples are not acquired to gain information on changes in petrophysical and acoustic properties of a given formation in the mechanical compaction domain.

Method and procedure

We conducted dry and brine-saturated mechanical compaction experiments using reconstituted mudstone and shale aggregates collected from drill cuttings of two exploration wells, 7220/10-1 (Salina discovery) and 7122/7-3 (Goliat field), located in SW Barents Sea. The washed and freeze-dried samples were characterized for mineralogical compositions, grain size distributions, and geochemical analyses. The experiments were conducted using a high-stress oedometer equipped with acoustic measurement transducers at the Norwegian Geotechnical Institute (NGI) laboratory. We investigated porosity evolution and velocity development (Vp and Vs) in the studied caprock samples. Subsequently, the laboratory measurements have been compared with previously published experimental data for synthetic aggregates of quartz-clay mixtures. The well log data from both exploration wells with different exhumation histories have also been used to investigate porosity- and velocity-depth trends of mudstone and shale stratigraphic successions in this area.

Key findings

The results show that:

- The laboratory-driven porosity- and velocity-depth trends of reconstituted aggregates agreed reasonably well with the in-situ natural condition recorded by wireline logs. Unlike compaction trends of the synthetic mixtures, both porosity and velocity (Vp and Vs) laboratory measurements show comparable values with the well log data in mechanical compaction domain. The deviation between laboratory and well log measurements is more visible for deeply buried sequences where deposits have experienced chemical compaction and cementation. As expected, the correlation between the rock properties becomes weaker with the increase of burial depth and temperature.

- It demonstrated that petrophysical and acoustic properties of argillaceous sediments may show notable variations as a function of burial within a sedimentary basin and even within a given formation. The ultrasonic velocity indicates that samples with the same porosity can have a broad range of velocity values. It suggests that a single empirical velocity-porosity relationship cannot successfully describe velocity of argillaceous rocks.

- The porosity-depth trends in shale and mudstone layers should be described by a bound that depends on the micro-scale properties and texture instead of a single line or equation. While the 100 % quartz silt defines the lower compressibility limit, the upper compressibility limit cannot be described by the synthetic binary mixtures.

- The introduced technique provides normal compaction trends (NCTs) for porosity, Vp and Vs of a given sedimentary formation in the mechanical compaction domain of sedimentary basins. Such NCTs can be used more reliably for uplift and exhumation estimations instead of NCTs derived from the synthetic binary mixtures.

Paper B: *Permeability and physical properties of semi-compacted fine-grained sediments – a laboratory study to constrain mudstone compaction trends*

Motivation and objectives

Decades of research on permeability evolution of fine-grained clastic sediments during burial have shown a broad range of variations in hydraulic conductivity of mudstones and shales, which can be expressed by linear-logarithmic porosity-permeability relationships with several orders of magnitude dispersion. Despite intensive published studies, the impact of individual constituents in terms of grain size and mineralogical composition on permeability is not thoroughly investigated. The primary objective was to examine whether the evolution of hydraulic and physical properties of naturally-driven reconstituted aggregates could be described and constrained by binary quartz-clay mixtures.

Method and procedure

We performed mechanical compaction of brine-saturated reconstituted borehole cuttings and synthetic mixtures of quartz-kaolinite and quartz-smectite in the laboratory to study changes in properties of the mudstone caprocks during burial. The experiments can simulate mechanical compaction of sediments in a normally compacted sedimentary basin with no superimposed tectonic forces before the onset of chemical compaction and cementation of the sediment framework. In addition to vertical permeability, physical and seismic properties, stress-dependence of permeability, and two-phase relative permeability were investigated.

Key findings

The following results focus exclusively on uncemented mudstones in the mechanical compaction domain of sedimentary basins:

- The experimental results indicate that grain size distribution and mineralogical composition impose control on the vertical permeability of fine-grained sediments. The specimens with lower clay-sized particles, higher silt-sized content, and higher sand-sized fractions show higher vertical permeability, in particular when sand-sized fractions are more than 10 %. The permeability decreases with the increase in the content of clay minerals, increase in carbonates, and the decrease in quartz and feldspar. The mentioned grain size– and mineralogy–permeability relationships, however, is not one-to-one. In other words, a higher or lower content of one constituent does not necessarily mean a higher or lower permeability. It underscores the influence of best-possible packing scenario on the permeability of fine-grained sediments.

- Although several studies have proposed that mudstones with similar content of size or mineralogy classes show similar permeability, two to three orders of magnitude scatter in permeability at a given value of grain size or mineralogy suggest that it may not be a universal observation. The synthetic quartz-clay mixtures demonstrate two orders of magnitude difference between the permeability of kaolinite- and smectite-rich specimens for the entire range of size and mineralogy classes. The clay mineral type, thus, also influences the porosity-permeability relationship of mudstones.

- A relatively well-constrained porosity-permeability bound is defined, where the pure quartz and quartz-smectite 15:85 compaction trends describe the maximum and minimum boundaries, respectively. Comparison of relationships between permeability, physical and seismic properties indicates that the reconstituted aggregates show higher elastic moduli and seismic properties, higher compaction, and lower total porosity compared to quartz-clay synthetic mixtures. As a result, the quartz-clay mixtures fail to provide bounds to constrain the broad range of variations in physical and seismic properties of reconstituted aggregates, and consequently natural mudstones.

- Seeking to approximate permeability of fine-grained sediments with a single macroscale equation may not provide a universal solution. Incorporating microstructure characteristics into the permeability models is a necessity because they control the macroscale fluid flow properties. In the absence of such information, the in-situ permeability of fine-grained sediments may not be reliably determined using geophysical techniques.

Paper C: *Compaction and mechanical strength of Middle Miocene mudstones in the Norwegian North Sea – The major seal for the Skade CO_2 storage reservoir*

Motivation and objectives

According to the CO_2 storage atlas of the Norwegian continental shelf (Halland et al., 2011), assessment of theoretical storage capacity has revealed that the Utsira–Skade deep saline aquifer has the highest storage capacity in the Norwegian North Sea. Contrasting to the reservoir units in the Skade Formation that are characterized in more details, the sealing quality and integrity of the caprock layer is quite uncertain. The Middle Miocene mudstones that serve as the primary seal sequence for the

Skade CO_2 storage reservoir are still in the mechanical compaction domain in the studied area, and no cementation is expected nor reported in this horizon. The physical properties of the caprock, therefore, are governed by initial textural and microstructural properties in addition to the effective stress level. This paper aimed to evaluate petrophysical, geomechanical, and rock physics properties of the caprock sequence.

Method and procedure

To evaluate caprock properties, we analyzed collected drill cuttings and measured well logs from well 16/4-1, in addition to an extensive well log database in the Northern North Sea. We carried out XRD analyses of whole-rock and clay mineral, grain size distribution, and electron microscopy of drill cuttings. To investigate changes in caprock properties, we performed experimental mechanical compaction of reconstituted drill cuttings. An extensive well log database was used to establish rock physics responses of the dominant mudstone facies. Moreover, geomechanical properties and brittleness indices of the studied caprock were evaluated. The lower bound of fracture pressure was also estimated in the well 16/4-1 for three different scenarios to provide a measure for maximum allowable pressure build-up during potential CO_2 injection in the Skade Formation.

Key findings

The results show that:

- The SEM analyses of drill cuttings identified an abundance of biogenic skeletal material mainly composed of silica in the Middle Miocene mudstones. The studied caprock is, thus, characterized as a mudstone rich in siliceous ooze.

- Seismic properties of mudstones in the Hordaland Group vary in a wide range, in which smectite-rich and siliceous ooze-rich intervals exhibit distinctive characteristics. While both facies show a similar range of Vp, the ooze-rich intervals have higher Vs than the smectite-rich horizons. As a result, smectite-rich mudstones have higher Vp/Vs ratio (around 3 to 3.5) compared to ooze-rich intervals (about 2.5). The oozy materials also cause a significant shift and a notable decrease in bulk density curves.

- The different scenarios for estimation of Vs showed that the ooze-rich intervals define the bound of highest brittleness in the Hordaland mudstones. The brittleness indices in well 16/4-1 indicate that the mineralogical composition-based definitions significantly overestimate brittleness compared to elastic-based definitions. While the caprock for the Skade CO_2 storage reservoir shows an overall ductility, the bottom 30 meters demonstrate an increased brittleness profile.

4.2 CO_2-induced salt precipitation (Paper D)

Paper D: *Effect of CO_2 phase states and flow rate on salt precipitation in shale caprocks – a microfluidic study*

Motivation and objectives

The CO_2 injection-induced salt precipitation has been the subject of rather comprehensive research. There are, however, knowledge gaps and inconsistencies in the previously reported results such as lack of a systematic study on the effect of CO_2 phase states and thermodynamic conditions on salt precipitation, or the inconsistencies regarding the extent and significance of salt precipitates and their impact on CO_2 percolation pathways. We, therefore, designed a series of pore- and microscale experiments to investigate the influence of thermodynamic (pressure-temperature) conditions and CO_2 phase states on the extent, distribution and precipitation pattern of salt crystals. We furthermore discussed a potential fracture healing mechanism, in which salt crystals partially or entirely block potential CO_2 leakage pathways in the caprock.

Method and procedure

We designed and fabricated a HPHT microfluidic pressure vessel to house micromodels made of geomaterial substrates. A fracture network pattern was laser-scribed on the organic-rich shales of the Draupne Formation, the primary caprock for the Smeaheia CO_2 storage site in Norway. The micromodels were saturated with NaCl solution before the experiments, and the brine saturation inside the fractures was replaced afterward with CO_2 under different phase states and injection rates. Pore-scale salt precipitation was monitored and digitally recorded under bright field imaging using a stereo microscope.

Key findings

The results show that:

- The salt crystals precipitate in two distinct forms: (a) large and semi-large (100-300 μm) single cubic crystals of halite in the aqueous phase; and (b) dense micrometer-sized (< 20 μm) halite crystals on the interface of rock and CO_2 stream.

- The CO_2 phase states and thermodynamic conditions were observed to control physics of salt precipitation as they influenced magnitude, distribution and precipitation pattern of localized salt accumulations. Injection of gaseous CO_2 resulted in higher salt precipitation compared to liquid and supercritical CO_2. The thermodynamic conditions influence the salt precipitation via water solubility in CO_2 (maximum water flux into CO_2 stream), and the balance between the imposed viscous forces and capillary-driven backflow.

- The CO_2 phase states also affect the relationship between injection rate, critical velocity, and the extent of precipitated salts. It is shown the higher the CO_2 injection flow rate, the lower the local salt coverage.

- The experimental observations showed micrometer-sized salt crystals that precipitate on the interface of fracture walls and CO_2 stream have the potential to partly or entirely block fracture apertures and consequently leakage pathways. The development of salt crystals toward the point where leakage begins, the affinity of salt bodies to become connected, and extent of accumulations suggest that salt precipitation during leakage of CO_2 can be considered as a fracture healing mechanism.

4.3 Geophysical monitoring of fracture flow (Paper E)

Paper E: *Effect of brine-CO_2 fracture flow on velocity and electrical resistivity of naturally fractured tight sandstones*

Motivation and objectives
Geophysical monitoring is a crucial measure to establish a reliable long-term CCS operation, and to track movements of the CO_2 plume. Several laboratory investigations have been performed to study geophysical properties of brine- and CO_2-saturated reservoir rock samples, and changes during fluid displacement of matrix saturation. Because pre-existing and induced fractures can play a role as CO_2 leakage pathways in the caprocks, it is important to assess changes in geophysical responses during brine-CO_2 fracture fluid displacement. There is, although, limited published research on the changes in geophysical properties of dominant brine-CO_2 fracture flow. The primary question in this study was whether it is possible to track CO_2 leakage along a fracture on a core-scale experiment? If yes, how are the sensitivity, detectability, and magnitude of changes in acoustic velocity and electrical resistivity?

Method and procedure

We conducted a core-scale flow-through experiment in the laboratory to measure the changes in acoustic velocity and electrical resistivity when CO_2 displaces brine out of the fracture. The stress dependence, hysteresis, and effect of fluid-rock interaction on fracture permeability were also studied. Moreover, x-ray microcomputed tomography imaged the fracture geometry and aperture before and after the experiments.

Key findings

The results show that:

- Stress dependence and hysteresis of fracture permeability indicated that at higher confining pressures significantly lower fracture permeabilities (even one order of magnitude) is expected compared with early stress levels. The pore pressure inside the fracture affects the fracture flow during loading and unloading stages. The gaseous CO_2 may cause a faster restoration of fracture permeability during the unloading stage than the liquid phase.

- Type of the injected fluid, and the consequent changes in volumetric strain because of the water injections-induced swelling and CO_2 injection-induced drying out resulted in a relative decrease and increase of permeability, respectively. The fracture permeability during injection of a non-interacting fluid (Marcol 52 oil) showed constant values.

- The axial P-wave velocity and axial electrical resistivity showed the highest sensitivity to saturation change compared with the axial S-wave velocity, radial Vp, and radial resistivity when liquid CO_2 displaced brine out the fracture. A minor reduction in P-wave anisotropy (Thomsen's epsilon parameter) and the resistivity anisotropy is observed during CO_2 injection. The radial resistivity sensors could detect the CO_2 front during drainage, but the radial Vp measurements could not capture the fluid displacement front.

- The marginal decreases of acoustic velocity (maximum 1.6 % for the axial Vp) compared with the 11 % increase in axial electrical resistivity suggest that in the case of potential CO_2 leakage, the use of electrical resistivity method has an advantage over the sole seismic method for monitoring CO_2 plume. Our further research showed that the crossplot of Vp versus electrical resistance could detect and help differentiate different fluid phases during the loading and unloading stages.

Chapter 5

Concluding Remarks

In this PhD dissertation, we have investigated properties of fine-grained siliciclastic caprocks with a particular focus on the evolution of mudstone properties in the mechanical compaction domain of sedimentary basins. We have also studied some of the processes that can happen because of the CO_2–brine–rock interactions during a potential CO_2 leakage through the top sealing layers. Moreover, laboratory experiments were carried out to see how geophysical monitoring techniques can detect fracture flow of CO_2 during an upward leakage of the CO_2 plume. For specific results and outcome of each study, the reader is referred to the chapter 4 or the respective papers. The dissertation, however, is distilled into the following three major findings:

The first presented topic is the evolution of rock properties during burial in fine-grained clastic sediments, with the focus on the mudstone and shale caprock sequences in the North Sea and the south-western Barents Sea. It showed significant variations in the petrophysical, geomechanical and rock physics properties of fine-grained argillaceous sediments during burial within a sedimentary basin, and even within a given formation. In other words, both depositional and compaction trends are determining factors for the understanding of geological trends. The papers demonstrate the importance of using and analyzing available resources (drill cuttings and well logs) to provide a realistic and comprehensive picture of the mudstone caprock properties. In particular, we showed that composition of rock constituents including bulk and clay mineralogy, grain size distribution, organic content, content of the biogenetic material, or in general microstructure characteristics of mudstones controls the macroscale properties. This is why it is important to emphasis on the study of borehole drill cuttings where core samples are not acquired. The laboratory compaction results of reconstituted aggregates and synthetic mixtures, in addition to the facies-based interpretation of wireline well logs provide valuable insights into the characteristics, compaction trends, and burial history of the studied caprocks.

The second addressed research topic was about salt precipitation and CO_2-induced drying-out in fractured shale caprocks. For the first time, to our knowledge, we introduce a conceptual framework that suggests salt precipitation is not only a near wellbore phenomenon but also a fracture sealing mechanism that can impede CO_2 leakage from the preexisting and induced fracture networks. We showed that precipitation of salt crystals is not limited to the residual brine saturation in the pore network, and significant amount of micrometer-sized salts are precipitating on the interface of rock and CO_2 flow pathway within the CO_2 phase. The thermodynamic (pressure-temperature) conditions and CO_2 phase states govern the physics of salt precipitation and directly impact on the magnitude, distribution and precipitation pattern of salt accumulations. The pore-scale microfluidic experiments also indicated where in the fracture network salt crystals precipitate and how separate accumulations distribute and develop, which can be of great significance for constructing clogging models for salt precipitation during CO_2 storage.

The third investigated topic considers a potential scenario, unfavorable though, in which the top sealing layer is leaking, and the CO_2-brine system is flowing through the fractured caprock. We performed a core-scale experiment to evaluate how much such a CO_2 leakage influence acoustic velocity and electrical resistivity, if any. It is shown the state of stress notably influences the fracture permeability in addition to the fluid-rock interaction. The fluid phase state impacts how fast or slow fracture permeability restores during unloading or injection-induced reactivation of the fracture network. In the core-scale fracture flow, geophysical sensors in axial and radial directions could detect CO_2-brine fluid substitution. However, acoustic velocity and electrical resistivity showed markedly different sensitivity and detectability, and underscored value of the electrical techniques. However, our further investigations revealed that collective consideration of Vp and electrical resistivity may provide the best outcome for monitoring of CO_2 storage sites.

5.1 Outlook

A great number of ideas, research questions, and need for further investigations were encountered during this PhD study. A couple of them that are not included in this dissertation are in progress, in preparation, or soon to be submitted to scholarly journals. Despite interest, and because I did not have the time to investigate any further, several research directions relating to this work, in my opinion, remain elusive and deserve further consideration:

- **Evolution of mudstones' properties:** The rock properties of caprock sequences in offshore Norway are affected by severe uplift and exhumation, particularly in the SW Barents Sea. While the majority of laboratory compaction studies have focused on the changes in mudstone properties during compaction, it can provide valuable insights to conduct a systematic and comprehensive study on how properties of fine-grained sediments change during decompression and unloading. Effect of micro-scale properties such as mineralogy and grain size, pre-compaction level, and loading and unloading rate need to be investigated. Moreover, it would be beneficial if the development of petrophysical, acoustic and elastic properties can be compared in uniaxial and triaxial configurations. Studying anisotropy and its changes during mechanical compaction both from triaxial results and under the microscope will be another direction.

- **CO_2-induced salt precipitation:** Pore-scale experiments can be performed to reduce uncertainties and resolve inconsistencies associated with the salt clogging models. Moreover, the effect of salt type and salt concentration on the extent and behavior of CO_2-induced micrometer-sized crystals need to be further assessed. How pore fluid contributes to salt precipitation in the intact or fractured real-rock reservoir sample can be studied over a range of thermodynamic conditions, injection rates, and salinities. The results should be then benchmarked to previous studies on glass microchips and from core flooding. Such a systematic approach may help to reduce the probability of injectivity impairment for a given storage site during the full-scale realization of CCS. Two directions would be exciting to follow regarding modeling of salt precipitation: (a) implementing first principles and pore-scale models, such as molecular dynamics and Lattice Boltzmann method, for capturing and further studying physics of salt precipitation and the governing mechanisms. Special attention should be given to clogging models while imposing proper boundary conditions. (b) field-scale simulation to test the introduced conceptual model about the ability of salt crystals to block CO_2 leakage pathways in the fractured caprocks. It is necessary, though, to use software packages that incorporate correct physics and thermodynamics for salt precipitation. Testing the conceptual model and comparing the predictions of salt precipitation using different equations of states (EoS) is another direction for field-scale simulations. Because of the dynamic and self-enhancing nature of salt precipitation, it is expected that current salt precipitation models based on volume balance approach can not provide realistic predictions.

- **Geophysical monitoring of fracture flow:** It is interesting to peruse several lines of core-scale experiments on the effect of pore pressure, CO_2 phase states, sole fracture flow versus simultaneous matrix and fracture flow, fracture aperture and fracture porosity, fracture stiffness on acoustic velocity and electrical resistivity with the application to injectivity, containment, and monitoring. However, it can provide more insights to conduct several numerical simulation studies based on the published laboratory results. In particular, core-scale simulation of dominant fracture flow (paper E) to compare the results from laboratory and simulation, and to benchmark the numerical model with the test results for constructing a numerical laboratory. Field-scale simulations need to be carried out to upscale the laboratory results and to study how such experimental efforts can be modified to provide better and more comprehensive results for large-scale modeling of CO_2 storage sites.

Bibliography

Adams, A.L., Germaine, J.T., Flemings, P.B., Day-Stirrat, R.J., 2013. *Stress induced permeability anisotropy of Resedimented Boston Blue Clay.* Water Resources Research 49, 6561-6571.

Alemu, B.L., Aagaard, P., Munz, I.A., Skurtveit, E., 2011. *Caprock interaction with CO_2: A laboratory study of reactivity of shale with supercritical CO_2 and brine.* Applied Geochemistry 26, 1975-1989.

Al-Tabbaa, A., Wood, D.M., 1987. *Some measurements of the permeability of kaolin.* Geotechnique 37, 499-514.

Amann-Hildenbrand, A., Bertier, P., Busch, A., Krooss, B.M., 2013. *Experimental investigation of the sealing capacity of generic clay-rich caprocks.* International Journal of Greenhouse Gas Control 19, 620-641.

André, L., Peysson, Y., Azaroual, M., 2014. *Well injectivity during CO2 storage operations in deep saline aquifers - Part 2: Numerical simulations of drying, salt deposit mechanisms and role of capillary forces.* International Journal of Greenhouse Gas Control 22, 301-312.

Aplin, A.C., Fleet, A.J., Macquaker, J.H.S., 1999. *Muds and mudstones: physical and fluid-flow properties.* Geological Society, London, Special Publications 158, 1.

Aplin, A.C., Macquaker, J.H.S., 2011. *Mudstone diversity: Origin and implications for source, seal, and reservoir properties in petroleum systems.* AAPG Bulletin 95, 2031-2059.

Athy, L.F., 1930. *Density, Porosity and Compaction of Sedimentary Rocks.* AAPG Bulletin 14, 1-24.

Avseth, P., Draege, A., van Wijingaarden, A.J., Johansen, T.A., Jørstad, A., 2008. *Shale rock physics and implications for AVO analysis: A North Sea demonstration.* Leading Edge (Tulsa, OK) 27, 788-797.

Avseth, P., Flesche, H., Van Wijngaarden, A.J., 2003. *AVO classification of lithology and pore fluids constrained by rock physics depth trends.* Leading Edge (Tulsa, OK) 22, 1004-1011.

Avseth, P., Mukerji, T., Mavko, G., 2005. *Quantitative seismic interpretation: Applying rock physics tools to reduce interpretation risk.* Cambridge University Press.

Avseth, P., Mukerji, T., Mavko, G., Dvorkin, J., 2010. *Rock-physics diagnostics of depositional texture, diagenetic alterations, and reservoir heterogeneity in high-porosity siliciclastic sediments and rocks - A review of selected models and suggested work flows.* Geophysics 75, X75A31-75A47.

Bacci, G., Durucan, S., Korre, A., 2013. *Experimental and numerical study of the effects of halite scaling on injectivity and seal performance during CO2 injection in saline aquifers.* Energy Procedia, pp. 3275-3282.

Bachrach, R., 2016. *Mechanical compaction in heterogeneous clastic formations from plastic-poroelastic deformation principles: theory and applications.* Geophysical Prospecting. 65, 724-735.

Bachu, S., 2000. *Sequestration of CO_2 in geological media: Criteria and approach for site selection in response to climate change.* Energy Conversion and Management 41, 953-970.

Bachu, S., 2015. *Review of CO_2 storage efficiency in deep saline aquifers.* International Journal of Greenhouse Gas Control 40, 188-202.

Baig, I., Faleide, J.I., Jahren, J., Mondol, N.H., 2016. *Cenozoic exhumation on the southwestern Barents Shelf: Estimates and uncertainties constrained from compaction and thermal maturity analyses.* Marine and Petroleum Geology 73, 105-130.

Baumann, G., Henninges, J., De Lucia, M., 2014. *Monitoring of saturation changes and salt precipitation during CO2 injection using pulsed neutron-gamma logging at the Ketzin pilot site.* International Journal of Greenhouse Gas Control 28, 134-146.

Beloborodov, R., Pervukhina, M., Lebedev, M., 2018. *Compaction trends of full stiffness tensor and fluid permeability in artificial shales.* Geophysical Journal International 212, 1687-1693.

Bennion, B., Bachu, S., 2005. *Relative permeability characteristics for supercritical CO_2 displacing water in a variety of potential sequestration zones in the western Canada sedimentary basin.* Proceedings - SPE Annual Technical Conference and Exhibition, pp. 859-873.

Bennion, B., Bachu, S., 2013. *Drainage and Imbibition Relative Permeability Relationships for Supercritical CO_2/Brine and H2S/Brine Systems in Intergranular Sandstone, Carbonate, Shale, and Anhydrite Rocks.* SPE Reservoir Evaluation & Engineering 11, 487-496.

Bennion, D.B., Bachu, S., 2008. *Drainage and imbibition relative permeability rela-*

tionships for supercritical CO_2/brine and H2S/brine systems in intergranular sandstone, carbonate, shale, and anhydrite rocks. SPE Reservoir Evaluation and Engineering 11, 487-496.

Benson, S.M., Cook, P., 2005. U*nderground Geological Storage*, in: Metz, B., Davidson, O., de Coninck, H., Loos, M., Meyer, L. (Eds.), *IPCC special report on Carbon Dioxide Capture and Storage.* Cambridge University Press, Cambridge, pp. 195-276.

Bernabé, Y., Fryer, D.T., Hayes, J.A., 1992. *The effect of cement on the strength of granular rocks.* Geophysical Research Letters 19, 1511-1514.

Berre, I., Doster, F., Keilegavlen, E., 2018. *Flow in Fractured Porous Media: A Review of Conceptual Models and Discretization Approaches.* Transport in Porous Media.

Bildstein, O., Kervévan, C., Lagneau, V., Delaplace, P., Crédoz, A., Audigane, P., Perfetti, E., Jacquemet, N., Jullien, M., 2010. *Integrative modeling of caprock integrity in the context of CO2 storage: Evolution of transport and geochemical properties and impact on performance and safety assessment.* Oil and Gas Science and Technology 65, 485-502.

Bjørlykke, K., 1998. *Clay mineral diagenesis in sedimentary basins - A key to the prediction of rock properties. Examples from the North Sea Basin.* Clay Minerals 33, 14-34.

Bjørlykke, K., 2015. *Compaction of sedimentary rocks: Shales, sandstones and carbonates*, In Petroleum Geoscience: From Sedimentary Environments to Rock Physics. Second Edition, pp. 351-360.

Bjørlykke, K., Aagaard, P., 1992. *Clay Minerals in North Sea Sandstones*, in: Houseknecht, D.W., Pittman, E.D. (Eds.), Origin, Diagenesis, and Petrophysics of Clay Minerals in Sandstones. SEPM Society for Sedimentary Geology.

Bjørlykke, K., Høeg, K., 1997. *Effects of burial diagenesis on stresses, compaction and fluid flow in sedimentary basins.* Marine and Petroleum Geology 14, 267-276.

Bohloli, B., Skurtveit, E., Grande, L., Titlestad, G.O., Børresen, M.H., Johnsen, Ø., Braathen, A., Braathen, A., 2014. *Evaluation of reservoir and cap-rock integrity for the longyearbyen CO_2 storage pilot based on laboratory experiments and injection tests.* Norsk Geologisk Tidsskrift 94, 171-187.

Brie, A., Pampuri, F., Marsala, A.F., Meazza, O., 1995. *Shear sonic interpretation in gas-bearing sands.* Proceedings - SPE Annual Technical Conference and Exhibition, pp. 701-710.

Cartwright, J., Huuse, M., Aplin, A., 2007. *Seal bypass systems.* AAPG Bulletin 91, 1141-1166.

Chermak, J.A., Rimstidt, J.D., 1990. *The hydrothermal transformation rate of kaolinite to muscovite/illite.* Geochimica et Cosmochimica Acta 54, 2979-2990.

Chilingarian, G.V., Rieke Iii, H.H., Donaldson, E.C., 1995. *Chapter 2 Compaction of argillaceous sediments*, Developments in Petroleum Science, pp. 47-164.

Chadwick, A., Williams, G., Delepine, N., Clochard, V., Labat, K., Sturton, S., Buddensiek, M., Dillen, M., Nickel, M., Lima, A., Arts, R., Neele, F., Rossi, G., 2010. *Quantitative analysis of time-lapse seismic monitoring data at the Sleipner CO2 storage operation.* The Leading Edge 29, 170-177.

Chen, H., Yang, S., Huan, K., Li, F., Huang, W., Zheng, A., Zhang, X., 2013. *Experimental study on monitoring CO2 sequestration by conjoint analysis of the P-wave velocity and amplitude.* Environ Sci Technol 47, 10071-10077.

Chuhan, F.A., Kjeldstad, A., Bjørlykke, K., Høeg, K., 2003. *Experimental compression of loose sands: Relevance to porosity reduction during burial in sedimentary basins.* Canadian Geotechnical Journal 40, 995-1011.

Cuadros, J., Linares, J., 1996. *Experimental kinetic study of the smectite-to-illite transformation.* Geochimica et Cosmochimica Acta 60, 439-453.

Daigle, H., Screaton, E.J., 2015. *Evolution of sediment permeability during burial and subduction.* Geofluids 15, 84-105.

Day-Stirrat, R.J., McDonnell, A., Wood, L.J., 2010. *Diagenetic and Seismic concerns associated with interpretation of deeply buried 'mobile shales'.* AAPG Memoir, 5-27.

De Segonzac, G.D., 1970. *The transformation of clay minerals during diagenesis and low-grade metamorphism: a review.* Sedimentology 15, 281-346.

Dewhurst, D.N., Aplin, A.C., Sarda, J.-P., Yang, Y., 1998. *Compaction-driven evolution of porosity and permeability in natural mudstones: An experimental study.* Journal of Geophysical Research: Solid Earth 103, 651-661.

Dewhurst, D.N., Aplin, A.C., Sarda, J.-P., 1999. *Influence of clay fraction on pore-scale properties and hydraulic conductivity of experimentally compacted mudstones.* Journal of Geophysical Research: Solid Earth 104, 29261-29274.

Downey, M.W., 1984. *Evaluating seals for hydrocarbon accumulations.* American Association of Petroleum Geologists Bulletin 68, 1752-1763.

Dutta, N.C., 2002. *Deepwater geohazard prediction using prestack inversion of large offset P-wave data and rock model.* Leading Edge (Tulsa, OK) 21, 193-198.

Falcon-Suarez, I., North, L., Amalokwu, K., Best, A., 2016. *Integrated geophysical and hydromechanical assessment for CO2storage: shallow low permeable reservoir sandstones*. Geophysical Prospecting 64, 828-847.

Falcon-Suarez, I., Papageorgiou, G., Chadwick, A., North, L., Best, A.I., Chapman, M., 2018. *CO2-brine flow-through on an Utsira Sand core sample: Experimental and modelling. Implications for the Sleipner storage field*. International Journal of Greenhouse Gas Control 68, 236-246.

Fawad, M., Mondol, N.H., Jahren, J., Bjørlykke, K., 2010. *Microfabric and rock properties of experimentally compressed silt-clay mixtures*. Marine and Petroleum Geology 27, 1698-1712.

Freed, R.L., Peacor, D.R., 1989. *Geopressured shale and sealing effect of smectite to illite transition*. American Association of Petroleum Geologists Bulletin 73, 1223-1232.

Gamage, K., Screaton, E., Bekins, B., Aiello, I., 2011. *Permeability–porosity relationships of subduction zone sediments*. Marine Geology 279, 19-36.

Gassmann, F., 1951. *Elastic waves through a packing of spheres*. GEOPHYSICS 16, 673-685.

Gaus, I., 2010. *Role and impact of CO_2–rock interactions during CO_2 storage in sedimentary rocks*. International Journal of Greenhouse Gas Control 4, 73-89.

Ghanizadeh, A., Gasparik, M., Amann-Hildenbrand, A., Gensterblum, Y., Krooss, B.M., 2013. *Lithological Controls on Matrix Permeability of Organic-rich Shales: An Experimental Study*. Energy Procedia 40, 127-136.

Gibbins, J., Chalmers, H., 2008. *Carbon capture and storage*. Energy Policy 36, 4317-4322.

Giles, M.R., Indrelid, S.L., James, D.M.D., 1998. *Compaction - the great unknown in basin modelling*, Geological Society Special Publication, pp. 15-43.

Giorgetti, G., Mata, M.P., Peacor, D.R., 2000. *TEM study of the mechanism of transformation of detrital kaolinite and muscovite to illite/smectite in sediments of the Salton Sea Geothermal Field*. European Journal of Mineralogy 12, 923-934.

Giorgis, T., Carpita, M., Battistelli, A., 2007. *2D modeling of salt precipitation during the injection of dry CO2 in a depleted gas reservoir*. Energy Conversion and Management 48, 1816-1826.

Gislason, S.R., Oelkers, E.H., 2014. *Carbon Storage in Basalt*. Science 344, 373.

Goulty, N.R., Sargent, C., Andras, P., Aplin, A.C., 2016. *Compaction of diagenetically altered mudstones – Part 1: Mechanical and chemical contributions*. Marine and Petroleum Geology 77, 703-713.

Griffith, C.A., Dzombak, D.A., Lowry, G.V., 2011. *Physical and chemical characteristics of potential seal strata in regions considered for demonstrating geological saline CO_2 sequestration.* Environmental Earth Sciences 64, 925-948.

Grude, S., Landrø, M., Dvorkin, J., 2014. *Pressure effects caused by CO2 injection in the Tubåen Fm., the Snøhvit field.* International Journal of Greenhouse Gas Control 27, 178-187.

Guyant, E., Han, W.S., Kim, K.Y., Park, M.H., Kim, B.Y., 2015. *Salt precipitation and CO2/brine flow distribution under different injection well completions.* International Journal of Greenhouse Gas Control 37, 299-310.

Haile, B.G., Klausen, T.G., Czarniecka, U., Xi, K., Jahren, J., Hellevang, H., 2018. *How are diagenesis and reservoir quality linked to depositional facies? A deltaic succession, Edgeøya, Svalbard.* Marine and Petroleum Geology 92, 519-546.

Halland, E., Bjørnestad, A., Magnus, C., Riis, F., Meling, I.M., Gjeldvik, I.T., Tappel, I.M., Mujezinović, J., Bjørheim, M., Rød, R.S., Pham, V.T.H., 2011. *CO_2 Storage Atlas of the Norwegian Continental Shelf.* Norwegian Petroleum Directorate.

Han, D.H., Batzle, M., 2006. *Velocities of deepwater reservoir sands.* Leading Edge (Tulsa, OK) 25, 460-466.

Hantschel, T., Kauerauf, A.I., 2009. *Fundamentals of basin and petroleum systems modeling.* Springer.

Hawkes, C.D., McLellan, P.J., Bachu, S., 2005. *Geomechanical Factors Affecting Geological Storage of CO2 in Depleted Oil and Gas Reservoirs.* PETSOC-05-10-05 44, 10.

Heath, J.E., Dewers, T.A., McPherson, B.J.O.L., Nemer, M.B., Kotula, P.G., 2012. *Pore-lining phases and capillary breakthrough pressure of mudstone caprocks: Sealing efficiency of geologic CO_2 storage sites.* International Journal of Greenhouse Gas Control 11, 204-220.

Hellevang, H., 2015. *Carbon capture and storage (CCS)*, Petroleum Geoscience: From Sedimentary Environments to Rock Physics, Second Edition, pp. 591-602.

Hildenbrand, A., Krooss, B.M., 2003. *CO_2 migration processes in argillaceous rocks: Pressure-driven volume flow and diffusion.* Journal of Geochemical Exploration 78-79, 169-172.

Holloway, S., 2005. *Underground sequestration of carbon dioxide - A viable greenhouse gas mitigation option.* Energy 30, 2318-2333.

Hower, J., Eslinger, E.V., Hower, M.E., Perry, E.A., 1976. *Mechanism of burial* *metamorphism of argillaceous sediment: 1. Mineralogical and chemical evidence.* Bulletin of the Geological Society of America 87, 725-737.

Hurter, S., Berge, J.G., Labregere, D., 2007. *Simulations for CO2 injection projects with Compositional Simulator, Offshore Europe.* Society of Petroleum Engineers, Aberdeen, Scotland, U.K., p. 7.

Iding, M., Ringrose, P., 2010. *Evaluating the impact of fractures on the performance of the In Salah CO2 storage site.* International Journal of Greenhouse Gas Control 4, 242-248.

IEA, 2016. International Energy Agency: *Energy Technology Perspectives.*

IPCC, 2014. *Climate Change 2014: Synthesis Report.* Contribution of Working Groups I, II and III to the Fifth Assessment Report of the Intergovernmental Panel on Climate Change. IPCC, Geneva, Switzerland, p. 151.

Jacops, E., Aertsens, M., Maes, N., Bruggeman, C., Krooss, B.M., Amann-Hildenbrand, A., Swennen, R., Littke, R., 2017. *Interplay of molecular size and pore network geometry on the diffusion of dissolved gases and HTO in Boom Clay.* Applied Geochemistry 76, 182-195.

Jeanne, P., Rutqvist, J., Wainwright, H.M., Foxall, W., Bachmann, C., Zhou, Q., Rinaldi, A.P., Birkholzer, J., 2016. *Effects of in situ stress measurement uncertainties on assessment of predicted seismic activity and risk associated with a hypothetical industrial-scale geologic CO_2 sequestration operation.* Journal of Rock Mechanics and Geotechnical Engineering 8, 873-885.

Ji, X., Tan, S.P., Adidharma, H., Radosz, M., 2005. *SAFT1-RPM approximation extended to phase equilibria and densities of CO_2-H_2O and CO_2-H_2O-NaCl systems.* Industrial and Engineering Chemistry Research 44, 8419-8427.

Kaldi, J.G., Atkinson, C.D., 1997. E*valuating seal potential: Example from the talang akar formation, offshore Northwest Java, Indonesia.* AAPG Memoir, 85-101.

Karadimitriou, N.K., Hassanizadeh, S.M., 2012. *A review of micromodels and their use in two-phase flow studies.* Vadose Zone Journal 11.

Kim, K.-Y., Han, W.S., Oh, J., Kim, T., Kim, J.-C., 2012. *Characteristics of Salt-Precipitation and the Associated Pressure Build-Up during CO2 Storage in Saline Aquifers.* Transport in Porous Media 92, 397-418.

Kim, M., Sell, A., Sinton, D., 2013. *Aquifer-on-a-Chip: Understanding pore-scale salt precipitation dynamics during CO2 sequestration.* Lab on a Chip 13, 2508-2518.

Kivior, T., Kaldi, J., Lang, S., 2002. *Seal potential in Cretaceous and Late Jurassic rocks of the Vulcan Sub-basin, Northwest Shelf Australia.* The APPEA Journal, 42(1), 203-224.

Knoll, M.D., Knight, R., 1994. *Relationships between Dielectric and Hydrogeologic Properties of Sand-Clay Mixtures*, Fifth International Conferention on Ground Penetrating Radar EAGE, Kitchener, Ontario, Canada.

Koochak Zadeh, M., Mondol, N.H., Jahren, J., 2016. *Experimental mechanical compaction of sands and sand-clay mixtures: a study to investigate evolution of rock properties with full control on mineralogy and rock texture.* Geophysical Prospecting 64, 915-941.

Lahann, R., 2004. *Impact of smectite diagenesis on compaction modeling and compaction equilibrium.* AAPG Memoir, 61-72.

Lashof, D.A., Ahuja, D.R., 1990. *Relative contributions of greenhouse gas emissions to global warming.* Nature 344, 529-531.

Lei, X., Xue, Z., 2009. *Ultrasonic velocity and attenuation during CO2 injection into water-saturated porous sandstone: Measurements using difference seismic tomography.* Physics of the Earth and Planetary Interiors 176, 224-234.

Leung, D.Y.C., Caramanna, G., Maroto-Valer, M.M., 2014. *An overview of current status of carbon dioxide capture and storage technologies.* Renewable and Sustainable Energy Reviews 39, 426-443.

Liu, F., Lu, P., Griffith, C., Hedges, S.W., Soong, Y., Hellevang, H., Zhu, C., 2012. *CO_2–brine–caprock interaction: Reactivity experiments on Eau Claire shale and a review of relevant literature.* International Journal of Greenhouse Gas Control 7, 153-167.

Loseth, H., Wensaas, L., Gading, M., Duffaut, K., Springer, M., 2011. *Can hydrocarbon source rocks be identified on seismic data?* Geology 39, 1167-1170.

Mallants, D., Marivoet, J., Sillen, X., 2001. *Performance assessment of the disposal of vitrified high-level waste in a clay layer.* Journal of Nuclear Materials 298, 125-135.

Marcussen, Ø., Faleide, J.I., Jahren, J., Bjørlykke, K., 2010. *Mudstone compaction curves in basin modelling: a study of Mesozoic and Cenozoic Sediments in the northern North Sea.* Basin Research 22, 324-340.

Matter, J.M., Kelemen, P.B., 2009. *Permanent storage of carbon dioxide in geological reservoirs by mineral carbonation.* Nature Geoscience 2, 837-841.

McCarty, J.P., 2001. *Ecological consequences of recent climate change.* Conservation Biology 15, 320-331.

Meinshausen, M., Meinshausen, N., Hare, W., Raper, S.C.B., Frieler, K., Knutti, R., Frame, D.J., Allen, M.R., 2009. *Greenhouse-gas emission targets for limiting global warming to 2°C*. Nature 458, 1158-1162.

Mesri, G., Olson, R.E., 1971. *Mechanisms controlling the permeability of clays.* Clays and Clay Minerals 19, 151-158.

Michael, K., Arnot, M., Cook, P., Ennis-King, J., Funnell, R., Kaldi, J., Kirste, D., Paterson, L., 2009. *CO_2 storage in saline aquifers I-Current state of scientific knowledge*, Energy Procedia, 1 ed, pp. 3197-3204.

Michael, K., Golab, A., Shulakova, V., Ennis-King, J., Allinson, G., Sharma, S., Aiken, T., 2010. *Geological storage of CO_2 in saline aquifers-A review of the experience from existing storage operations.* International Journal of Greenhouse Gas Control 4, 659-667.

Milliken, K.L., Day-Stirrat, R.J., 2013. *Cementation in mudrocksz: Brief review with examples from cratonic basin mudrocks.* AAPG Memoir, 133-150.

Miri, R., Aagaard, P., Hellevang, H., 2014. *Examination of CO_2-SO_2 solubility in water by SAFT1. Implications for CO_2 transport and storage.* Journal of Physical Chemistry B 118, 10214-10223.

Miri, R., van Noort, R., Aagaard, P., Hellevang, H., 2015. *New insights on the physics of salt precipitation during injection of CO2 into saline aquifers.* International Journal of Greenhouse Gas Control 43, 10-21.

Miri, R., Hellevang, H., 2016. *Salt precipitation during CO_2 storage—A review.* International Journal of Greenhouse Gas Control 51, 136-147.

Mondol, N.H., Bjørlykke, K., Jahren, J., Høeg, K., 2007. *Experimental mechanical compaction of clay mineral aggregates—Changes in physical properties of mudstones during burial.* Marine and Petroleum Geology 24, 289-311.

Mondol, N.H., 2009. *Porosity and permeability development in mechanically compacted silt-kaolinite mixtures*, SEG Technical Program Expanded Abstracts, pp. 2139-2143.

Muller, N., Qi, R., Mackie, E., Pruess, K., Blunt, M.J., 2009. *CO2 injection impairment due to halite precipitation*, Energy Procedia, 1 ed, pp. 3507-3514.

Nadeau, P.H., Peacor, D.R., Yan, J., Hillier, S., 2002. *I-S precipitation in pore space as the cause of geopressuring in Mesozoic mudstones, Egersund Basin, Norwegian continental shelf.* American Mineralogist 87, 1580-1589.

Nakagawa, S., Kneafsey, T.J., Daley, T.M., Freifeld, B.M., Rees, E.V., 2013. *Laboratory seismic monitoring of supercritical CO2flooding in sandstone cores using the*

Split Hopkinson Resonant Bar technique with concurrent x-ray Computed Tomography imaging. Geophysical Prospecting 61, 254-269.

Nakatsuka, Y., Xue, Z., Garcia, H., Matsuoka, T., 2010. *Experimental study on CO2 monitoring and quantification of stored CO2 in saline formations using resistivity measurements.* International Journal of Greenhouse Gas Control 4, 209-216.

Nelson, C., Evans, J., Sorensen, J., Steadman, E., Harju, J., 2005. *FACTORS AFFECTING THE POTENTIAL FOR CO2 LEAKAGE FROM GEOLOGIC SINKS.*

Nooraiepour, M., Bohloli, B., Park, J., Sauvin, G., Skurtveit, E., Mondol, N., 2018a. *Effect of brine-CO_2 fracture flow on velocity and electrical resistivity of naturally fractured tight sandstones.* GEOPHYSICS 83, WA37-WA48.

Nooraiepour, M., Fazeli, H., Miri, R., Hellevang, H., 2018b. *Effect of CO_2 Phase States and Flow Rate on Salt Precipitation in Shale Caprocks—A Microfluidic Study.* Environmental Science & Technology 52, 6050-6060.

Nooraiepour, M., Haile, B.G., Hellevang, H., 2017a. *Compaction and mechanical strength of Middle Miocene mudstones in the Norwegian North Sea – The major seal for the Skade CO_2 storage reservoir.* International Journal of Greenhouse Gas Control 67, 49-59.

Nooraiepour, M., Mondol, N.H., Hellevang, H., Bjørlykke, K., 2017b. *Experimental mechanical compaction of reconstituted shale and mudstone aggregates: Investigation of petrophysical and acoustic properties of SW Barents Sea cap rock sequences.* Marine and Petroleum Geology 80, 265-292.

Oh, J., Kim, K.-Y., Han, W.S., Kim, T., Kim, J.-C., Park, E., 2013. *Experimental and numerical study on supercritical CO2/brine transport in a fractured rock: Implications of mass transfer, capillary pressure and storage capacity.* Advances in Water Resources 62, 442-453.

Ott, H., Andrew, M., Snippe, J., Blunt, M.J., 2014. *Microscale solute transport and precipitation in complex rock during drying.* Geophysical Research Letters 41, 8369-8376.

Ott, H., de Kloe, K., van Bakel, M., Vos, F., van Pelt, A., Legerstee, P., Bauer, A., Eide, K., van der Linden, A., Berg, S., Makurat, A., 2012. *Core-flood experiment for transport of reactive fluids in rocks.* Rev Sci Instrum 83, 084501.

Ott, H., Roels, S.M., de Kloe, K., 2015. *Salt precipitation due to supercritical gas injection: I. Capillary-driven flow in unimodal sandstone.* International Journal of Greenhouse Gas Control 43, 247-255.

Peysson, Y., André, L., Azaroual, M., 2014. *Well injectivity during CO2 storage* *operations in deep saline aquifers-Part 1: Experimental investigation of drying effects, salt precipitation and capillary forces.* International Journal of Greenhouse Gas Control 22, 291-300.

Porter, M.L., Jiménez-Martínez, J., Martinez, R., McCulloch, Q., Carey, J.W., Viswanathan, H.S., 2015. *Geo-material microfluidics at reservoir conditions for subsurface energy resource applications.* Lab on a Chip 15, 4044-4053.

Pruess, K., Müller, N., 2009. *Formation dry-out from CO2 injection into saline aquifers: 1. Effects of solids precipitation and their mitigation.* Water Resources Research 45.

Riahi, K., Rao, S., Krey, V., Cho, C., Chirkov, V., Fischer, G., Kindermann, G., Nakicenovic, N., Rafaj, P., 2011. *RCP 8.5-A scenario of comparatively high greenhouse gas emissions.* Climatic Change 109, 33-57.

Roels, S.M., Ott, H., Zitha, P.L.J., 2014. *micro-CT analysis and numerical simulation of drying effects of CO2 injection into brine-saturated porous media.* International Journal of Greenhouse Gas Control 27, 146-154.

Root, T.L., Price, J.T., Hall, K.R., Schneider, S.H., Rosenzweig, C., Pounds, J.A., 2003. *Fingerprints of global warming on wild animals and plants.* Nature 421, 57-60.

Rutqvist, J., 2015. *Fractured rock stress-permeability relationships from in situ data and effects of temperature and chemical-mechanical couplings.* Geofluids 15, 48-66.

Rutqvist, J., 2012. *The Geomechanics of CO_2 Storage in Deep Sedimentary Formations.* Geotechnical and Geological Engineering 30, 525-551.

Rutqvist, J., Birkholzer, J., Cappa, F., Tsang, C.F., 2007. *Estimating maximum sustainable injection pressure during geological sequestration of CO_2 using coupled fluid flow and geomechanical fault-slip analysis.* Energy Conversion and Management 48, 1798-1807.

Rutqvist, J., Tsang, C.-F., 2002. *A study of caprock hydromechanical changes associated with CO_2-injection into a brine formation.* Environmental Geology 42, 296-305.

Saffer, D.M., Silver, E.A., Fisher, A.T., Tobin, H., Moran, K., 2000. *Inferred pore pressures at the Costa Rica subduction zone: Implications for dewatering processes.* Earth and Planetary Science Letters 177, 193-207.

Santagata, M., Kang, Y.I., 2007. *Effects of geologic time on the initial stiffness of clays.* Engineering Geology 89, 98-111.

Schlömer, S., Krooss, B.M., 1997. *Experimental characterisation of the hydrocarbon sealing efficiency of cap rocks.* Marine and Petroleum Geology 14, 565-580.

Schneider, J., Flemings, P.B., Day-Stirrat, R.J., Germaine, J.T., 2011. *Insights into* *pore-scale controls on mudstone permeability through resedimentation experiments.* Geology 39, 1011-1014.

Screaton, E.J., Wuthrich, D.R., Dreiss, S.J., 1990. *Permeabilities, fluid pressures, and flow rates in the Barbados Ridge complex.* Journal of Geophysical Research 95, 8997-9007.

Seah, T.H., 1990. *Anisotropy of resedimented Boston Blue Clay*, Department of Civil Engineering. Massachusetts Institute of Technology, Cambridge, USA, p. 1065.

Sheahan, T.C., 1991. *An experimental study of the time-dependent undrained shear behavior of resedimented clay using automated stress path triaxial equipment*, Department of Civil Engineering. Massachusetts Institute of Technology, Cambridge, USA, p. 952.

Shine, K.P., Fuglestvedt, J.S., Hailemariam, K., Stuber, N., 2005. *Alternatives to the Global Warming Potential for comparing climate impacts of emissions of greenhouse gases.* Climatic Change 68, 281-302.

Shukla, R., Ranjith, P., Haque, A., Choi, X., 2010. *A review of studies on CO_2 sequestration and caprock integrity.* Fuel 89, 2651-2664.

Smith, J., Durucan, S., Korre, A., Shi, J.Q., 2011. *Carbon dioxide storage risk assessment: Analysis of caprock fracture network connectivity.* International Journal of Greenhouse Gas Control 5, 226-240.

Song, J., Zhang, D., 2013. *Comprehensive review of caprock-sealing mechanisms for geologic carbon sequestration.* Environ Sci Technol 47, 9-22.

Storvoll, V., Bjørlykke, K., Mondol, N.H., 2005. *Velocity-depth trends in Mesozoic and Cenozoic sediments from the Norwegian Shelf.* AAPG Bulletin 89, 359-381.

Storvoll, V., Brevik, I., 2008. *Identifying time, temperature, and mineralogical effects on chemical compaction in shales by rock physics relations.* The Leading Edge 27, 750-756.

Sun, Y., Li, Q., Yang, D., Liu, X., 2016. *Laboratory core flooding experimental systems for CO2 geosequestration: An updated review over the past decade.* Journal of Rock Mechanics and Geotechnical Engineering 8, 113-126.

Tang, Y., Yang, R., Du, Z., Zeng, F., 2015. *Experimental Study of Formation Damage Caused by Complete Water Vaporization and Salt Precipitation in Sandstone Reservoirs.* Transport in Porous Media 107, 205-218.

Tanikawa, W., Hirose, T., Mukoyoshi, H., Tadai, O., Lin, W., 2013. *Fluid transport properties in sediments and their role in large slip near the surface of the plate* *boundary fault in the Japan Trench.* Earth and Planetary Science Letters 382, 150-160.

Teige, G.M.G., Hermanrud, C., Rueslåtten, H.G., 2010. *Membrane seal leakage in non-fractured caprocks by the formation of oil-wet flow paths.* Journal of Petroleum Geology 34, 45-52.

Thyberg, B., Jahren, J., 2011. *Quartz Cementation in Mudstones: Sheet-Like Quartz Cement from Clay Mineral Reactions during Burial.* Petroleum Geoscience 17, 53-63.

Thyberg, B., Jahren, J., Winje, T., Bjørlykke, K., Faleide, J.I., Marcussen, Ø., 2010. *Quartz cementation in Late Cretaceous mudstones, northern North Sea: Changes in rock properties due to dissolution of smectite and precipitation of micro-quartz crystals.* Marine and Petroleum Geology 27, 1752-1764.

Torsæter, M., Cerasi, P., 2018. *Geological and geomechanical factors impacting loss of near-well permeability during CO2 injection.* International Journal of Greenhouse Gas Control 76, 193-199.

van de Kamp, P.C., 2008. *Smectite-illite-muscovite transformations, quartz dissolution, and silica release in shales.* Clays and Clay Minerals 56, 66-81.

Vasseur, G., Djeran-Maigre, I., Grunberger, D., Rousset, G., Tessier, D., Velde, B., 1995. *Evolution of structural and physical parameters of clays during experimental compaction.* Marine and Petroleum Geology 12, 941-954.

Verma, A., Pruess, K., 1988. *Thermohydrological conditions and silica redistribution near high-level nuclear wastes emplaced in saturated geological formations.* Journal of Geophysical Research 93, 1159-1173.

Vavra, C.L., Kaldi, J.G., Sneider, R.M., 1992. *Geological applications of capillary pressure: a review.* American Association of Petroleum Geologists Bulletin 76, 840-850.

Velde, B., 1996. *Compaction trends of clay-rich deep sea sediments.* Marine Geology 133, 193-201.

Vernik, L., Nur, A., 1992. *Petrophysical classification of siliciclastics for lithology and porosity prediction from seismic velocities.* American Association of Petroleum Geologists Bulletin 76, 1295-1309.

Wang, Y., Mackie, E., Rohan, J., Luce, T., Knabe, R.J., Appel, M., 2009. *Experimental study on halite precipitation during CO2 sequestration*, International Symposium of the Society of Core Analysts. Society of Core Analysts, Noordwijk, The Netherlands.

Watts, N.L., 1987. *Theoretical aspects of cap-rock and fault seals for single- and two-phase hydrocarbon columns.* Marine and Petroleum Geology 4, 274-307.

Wentworth, C.K., 1922. *A Scale of Grade and Class Terms for Clastic Sediments.* The Journal of Geology 30, 377-392.

White, J.A., Foxall, W., 2016. *Assessing induced seismicity risk at CO_2 storage projects: Recent progress and remaining challenges.* International Journal of Greenhouse Gas Control 49, 413-424.

Winkler, K.W., 1983. *Contact stiffness in granular porous materials: Comparison between theory and experiment.* Geophysical Research Letters 10, 1073-1076.

Wollenweber, J., Alles, S., Busch, A., Krooss, B.M., Stanjek, H., Littke, R., 2010. *Experimental investigation of the CO_2 sealing efficiency of caprocks.* International Journal of Greenhouse Gas Control 4, 231-241.

Wurdemann, H., Möller, F., Kühn, M., Heidug, W., Christensen, N.P., Borm, G., Schilling, F.R., 2010. *CO_2SINK—From site characterisation and risk assessment to monitoring and verification: One year of operational experience with the field laboratory for CO_2 storage at Ketzin, Germany.* International Journal of Greenhouse Gas Control 4, 938-951.

Yamabe, H., Tsuji, T., Liang, Y., Matsuoka, T., 2016. *Influence of fluid displacement patterns on seismic velocity during supercritical CO2 injection: Simulation study for evaluation of the relationship between seismic velocity and CO2 saturation.* International Journal of Greenhouse Gas Control 46, 197-204.

Yang, Y., Aplin, A.C., 2007. *Permeability and petrophysical properties of 30 natural mudstones.* Journal of Geophysical Research 112.

Yin, H., Zhou, J., Jiang, Y., Xian, X., Liu, Q., 2016. *Physical and structural changes in shale associated with supercritical CO2 exposure.* Fuel 184, 289-303.

Zeidouni, M., Pooladi-Darvish, M., Keith, D., 2009. *Sensitivity Analysis of Salt Precipitation and CO2-Brine Displacement in Saline Aquifers.* Society of Petroleum Engineers.

Zimmer, M.A., Prasad, M., Mavko, G., Nur, A., 2007. *Seismic velocities of unconsolidated sands: Part 2 - Influence of sorting- and compaction-induced porosity variation.* Geophysics 72, E15-E25.

Part II

Papers

Part III

Appendices